Electronic Supporting Information

Dual Application of a Fluorene Based Switch-On Chemosensor for Mercury and Glutathione Sensing in Water: Analyte Recognition Triggered Self-Assembly

Megha Basak, Gopal Das*

Department of Chemistry, Indian Institute of Technology Guwahati, Assam 781039, India,
gdas@iitg.ac.in

Experimental Section

General Information and Materials

All the reagents, solvents, starting materials, different metal salts and amino acids were procured from commercial purveyors and were used as received. All were of reagent grade. The solvents used were HPLC grade. For N.M.R. analyses, deuterated solvent [$(CD_3)_2SO$] was purchased from Sigma-Aldrich.

The UV-Visible absorption spectra were archived on a Perkin-Elmer Lamda-750 UV-Vis spectrophotometer using 10 mm path length quartz cuvettes in 250-700 nm wavelengths. Baseline correction was applied for all spectra.

Fluorescence emission spectra were documented on a Horiba Fluoromax-4 spectrofluorometer using a 1 cm path length of quartz cuvettes having a slit width of 3 nm at 298 K.

High-resolution mass spectrometry of $\mathbf{L_1}$, $\mathbf{L_2}$, $\mathbf{L_3}$, $\mathbf{L_1}$-Hg^{2+} and $\mathbf{L_1}$-GSH was carried out on a Waters Q-ToF Premier mass spectrometer.

The solution-phase ^1H and ^{13}C Nuclear Magnetic Resonance spectra were recorded at 500 MHz using a Bruker Advances 500NMR instrument. The chemical shifts were reported in parts per million (ppm) with the deuterated solvents. The following abbreviations are used to delineate spin multiplicities in ^1H NMR spectra: s = singlet; d = doublet; t = triplet; q= quartet, m = multiplet.

Synthetic procedure of $\mathbf{L_1}$, $\mathbf{L_2}$ and $\mathbf{L_3}$

To a stirring solution (10 mmol, 1.96 g) of 2,7diaminofluorene in methanol (10mL), 4-diethylamino salicaldehyde (25 mmol, 4.8 g) in 10mL methanol was added and refluxed overnight. Condensation of these two reactants resulted a Schiff base product, filtered and collected after frequent washing with cold methanol. The gradual addition of $NaBH_4$ in ice-cold condition reduced the Schiff base in its methanolic solution. After the reaction, water was added dropwise to the reaction mixture and extracted with CH_2Cl_2. The organic phase was separated and concentrated under reduced pressure to procure the dark brown product $\mathbf{L_1}$. Similar synthetic procedure was followed introducing salicaldehyde (25 mmol, 2.6g) and 4-dimethylamino benzaldehyde (25 mmol, 3.72 g) respectively to procure $\mathbf{L_2}$ and $\mathbf{L_3}$. $\mathbf{L_1}$, $\mathbf{L_2}$ and $\mathbf{L_3}$ were well characterized by ESI-MS, ^1H NMR, ^{13}C NMR, FT-IR analysis.

Characterization data of L_1: Calculated Yield =75%. ESI-MS (positive mode, m/z) calculated for $C_{35}H_{42}N_4O_2$ $[M+H]^+$: 551.3580. Found: 551.3582. ^1H NMR of **L_1** (500 MHz, DMSO-d_6, δ ppm): 8.75 (s, 1H), 7.23-7.25 (d, 1H), 6.76-6.79 (d, 1H), 6.68 (s, 1H), 6.47-6.49(d, 1H), 6.15 (s, 1H), 6.02-6.04 (d, 1H), 4.89 (s, 2H), 3.57 (s, 1H), 3.18-3.24 (m, 4H), 1.02-1.06(t, 6H). ^{13}C NMR (150 MHz, DMSO-d_6, δ ppm): 156.12, 147.15, 146.44, 143.17, 131.28, 131.21, 130.99, 118.58, 112.73, 111.05, 110.72, 103.46, 99.48, 43.99, 36.29, 15.17, 12.68. FT-IR (KBr pellets, cm-1): 3367 (O-H), 3307 (N-H), 2963 (Aromatic C-H), 1619(N-H bending), 1466 (Aromatic ring C=C stretching), 1256 (C-N stretch), 804 (N-H wagging).

Characterization data of L_2: Calculated Yield =73%. ESI-MS (positive mode, m/z) calculated for $C_{27}H_{24}N_2O_2$ $[M+H]^+$: 409.1916. Found: 409.1957. ^1H NMR of **L_1** (500 MHz, DMSO-d_6, δ ppm): 9.51 (s, 1H), 7.26-7.28 (d, 1H), 7.19-7.21 (d, 1H), 7.01-7.05 (t, 1H), 6.80-6.82(d, 1H), 6.73 (s, 1H), 6.70-6.71 (d, 1H), 6.50 (s, 1H), 5.84 (s, 1H), 4.20 (s, 2H), 3.57(s, 1H). ^{13}C NMR (150 MHz, DMSO-d_6, δ ppm): 155.44, 143.53, 132.83, 128.67, 127.87, 120.01, 119.53, 119.21, 118.95, 111.80, 116.98, 115.26, 31.74, 29.47. FT-IR (KBr pellets, cm-1): 3283 (O-H), 2920 (N-H), 2851 (Aromatic C-H), 1614(N-H bending), 1461 (Aromatic ring C=C stretching), 1245(C-N stretch), 813 (N-H wagging).

Characterization data of L_3: Calculated Yield =75%. ESI-MS (positive mode, m/z) calculated for $C_{31}H_{34}N_4$ $[M]^+$: 462.2874 Found: 462.2880. ^1H NMR of **L_1** (500 MHz, DMSO-d_6, δ ppm): 7.62-7.65 (d, 1H), 7.21-7.22 (d, 1H), 7.13 (s, 1H), 6.73-6.75 (d, 1H), 6.66(s, 1H), 6.62-6.64 (d, 1H), 6.46 (s, 1H), 4.09 (s, 1H), 2.98 (s, 3H. ^{13}C NMR (150 MHz, DMSO-d_6, δ ppm): 154.68, 142.92, 143.48, 128.55, 124.88, 118.92, 112.91, 111.50, 109.63, 46.95, 40.70, 36.54. FT-IR (KBr pellets, cm-1): 2920 (N-H), 2850 (Aromatic C-H), 1607(N-H bending), 1464 (Aromatic ring C=C stretching), 1226 (C-N stretch), 805 (N-H wagging).

General Procedure for UV-VIS and Fluorescence Spectroscopic Studies

Stock solutions of different metals and amino acid solutions (50×10^{-3}mol L^{-1}) were prepared in water. Stock solution of **L_1** , **L_2** and **L_3** (1×10^{-3}mol L^{-1}) were prepared in DMSO. For fluorescence selectivity experiments, the solution of probes was then diluted to 2×10^{-6} mol L^{-1} with Millipore water by taking only 4μL of stock solution and making the final volume 2 mL. In fluorescence titration experiments, a quartz optical cell of 10mm pathlength was filled with a 2.0 mL solution of **L_1** to which various analytes were gradually added using a micropipette. For fluorescence measurements, **L_1** was excited at 315 nm, and emission was procured from 335 nm to 650 nm.

Estimation of the Apparent Binding Constant

The ligand $\mathbf{L_1}$ with an effective concentration of 2μM was used for the fluorescence emission titration studies with GSH solution in aqueous medium. The effective GSH concentrations were varied between 0 and 20 equivalent for this titration. The apparent binding constants for the formation of the respective complexes were evaluated using the Benesi–Hildebrand (B–H) plot (**Equation 1**). [1-2]

$$1/(I-I_0) = 1/\{K(I_{max}-I_0)\ C\} + 1/(I_{max}-I_0) \qquad (1)$$

I_0 is the emission intensity of $\mathbf{L_1}$ at λ = 384 nm, I is the observed emission intensity at the particular wavelength in the presence of a certain concentration of the analyte (C), I_{max} is the maximum emission intensity value that was obtained at λ = 420 nm during titration with varying analyte concentration, K is the apparent binding constant (M^{-1}) and was determined from the slope of the linear plot, and C is the concentration of the GSH added during titration studies.

Detection Limit

The detection limit was evaluated based on the fluorescence titration changes for Hg^{2+} and GSH independently. $\mathbf{L_1}$'s fluorescence emission spectrum was computed ten times, and the standard deviation of the blank measurement was obtained. The fluorescence emission at 414 nm and 420 nm was plotted as a concentration of Hg^{2+} and GSH to gain the slope. The detection limits were calculated using the following equation:

$$\text{Detection limit} = 3\sigma/k \qquad (2)$$

where σ is the standard deviation of blank measurement, and k is the slope between the fluorescence emission intensity versus [analyte]. The conversion to ppb unit was done considering Mol. Wt. of mercury 200.59 $gmol^{-1}$ and GSH 307.32 $gmol^{-1}$.

Field Emission Scanning Electron Microscope (FESEM) Studies

Morphology of $\mathbf{L_1}$, $\mathbf{L_1}$-Hg^{2+} complex was imaged separately using Gemini 300 FESEM (Carl Zeiss) instrument. The samples were prepared by drop-casting (2μM), the DMSO/Water mixture on Al-foil wrapped coverslip, then coated with Au and dried under vacuum before the imaging.

Fluorescence Microscopy

The freshly prepared samples of $\mathbf{L_1}$ (2 μM), $\mathbf{L_1}$-Hg^{2+} complex (**Probe 1** mixed with 50 equivalents of mercury(II) salt) and $\mathbf{L_1}$-GSH complex (**Probe 1** mixed with 50 equivalents of GSH) glass slide and were entirely dried at room temperature, followed by image acquisition

using a Fluorescence microscope (Eclipse Ti-U, Nikon, U.S.A.) with a blue filter. In plant tissue and gram seed imaging, leaf, stem and cotyledons of gram seed were dissected. Then the 30μm sections were sliced and placed on a glass slide to capture images by fluorescence microscope.

Measurement of fluorescence lifetime

Fluorescence lifetimes were evaluated utilizing the time-correlated single-photon counting (TCSPC) method in the Edinburgh Instrument Life-Spec II spectrometer. The samples (**L_1**, **L_1**-Hg^{2+} and **L_1**-GSH) were excited at 315 nm keeping the emission wavelength at 414 nm and 420 nm using a pulsed diode laser. The fluorescence decays were surveyed by the re-convolution method using the FAST software provided by Edinburgh Instruments.

Photoluminescence Quantum Yield

We had pursued the Petite Integrating Sphere method to determine the quantum yield by Horiba Jobin Yvon Fluoromax-4 Spectrofluorometer. It was determined in 100% aqueous medium for **L_1** (2 μM), **L_1**-Hg^{2+} complex (**L_1** mixed with 50 equivalents of Hg^{2+}) and **L_1**-GSH complex (**L_1** mixed with 50 equivalents of GSH) keeping λ_{ex} at 315 nm. To determine the quantum yield, the equation we employed was (as per the instruction written on the official website of Horiba),

$$\Phi = [(E_c - E_a) / (L_a - L_c)] \qquad (3)$$

Where E_c = Emission of the sample, E_a = Emission of the blank, L_c = Scatter of the sample & L_a = Scatter of the blank.

Theoretical investigations (DFT study)

DFT optimizations of **L_1** , **L_1**-GSH and **L_1**-Hg^{2+} complex were accomplished with the exchange correlation function B3LYP-D3(http://www.gaussian.com/g_tech/g_ur/k_dft.htm) and the basis set 6-31G (d,p) for C,H, N and O atoms and LANL2DZ for Hg atoms incorporating in the Gaussian 09 package.[3] TDDFT computations were then carried out based on the optimized ground state geometries using the Time dependent Self-Consistent Field (TD-SCF) method.

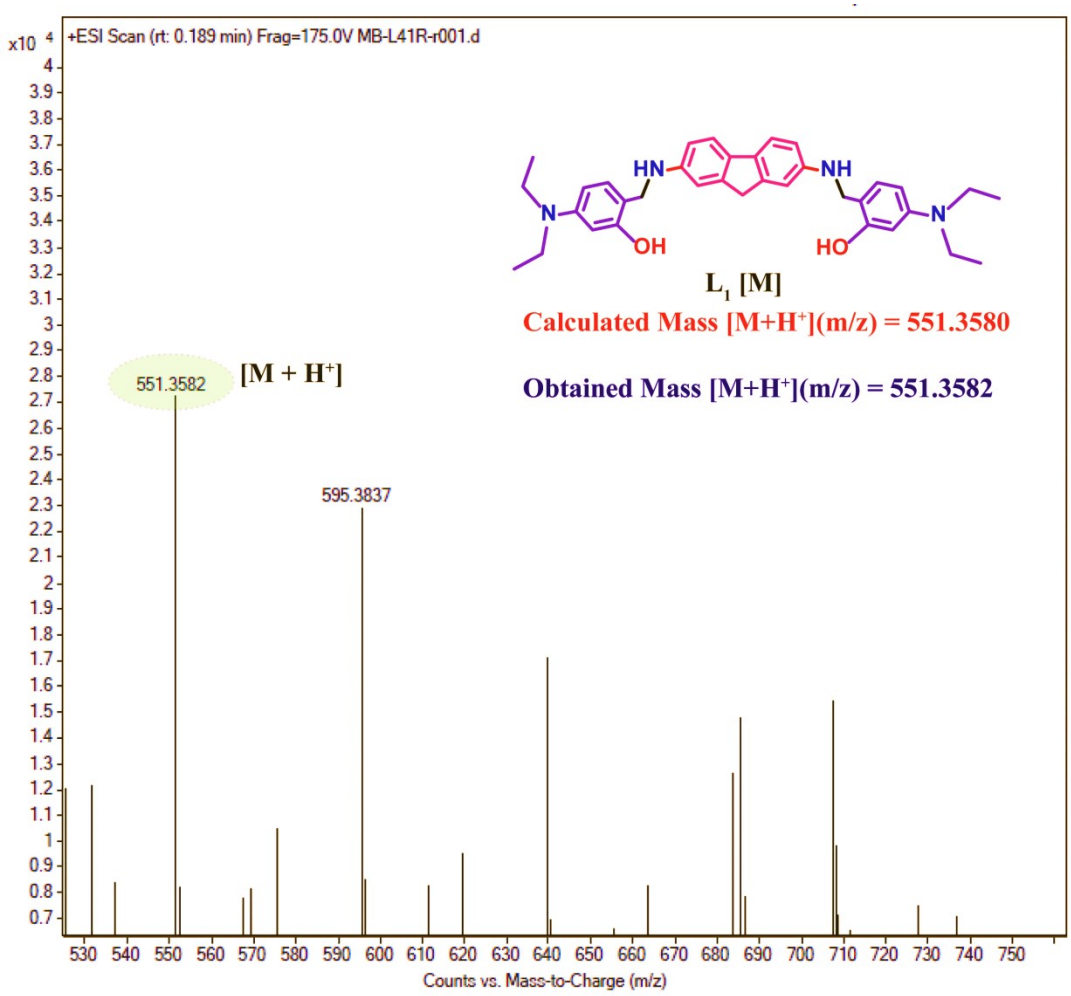

Figure S1: ESI-MS spectra of $\mathbf{L_1}$ in 1:1 water-acetonitrile in positive ionization mode.

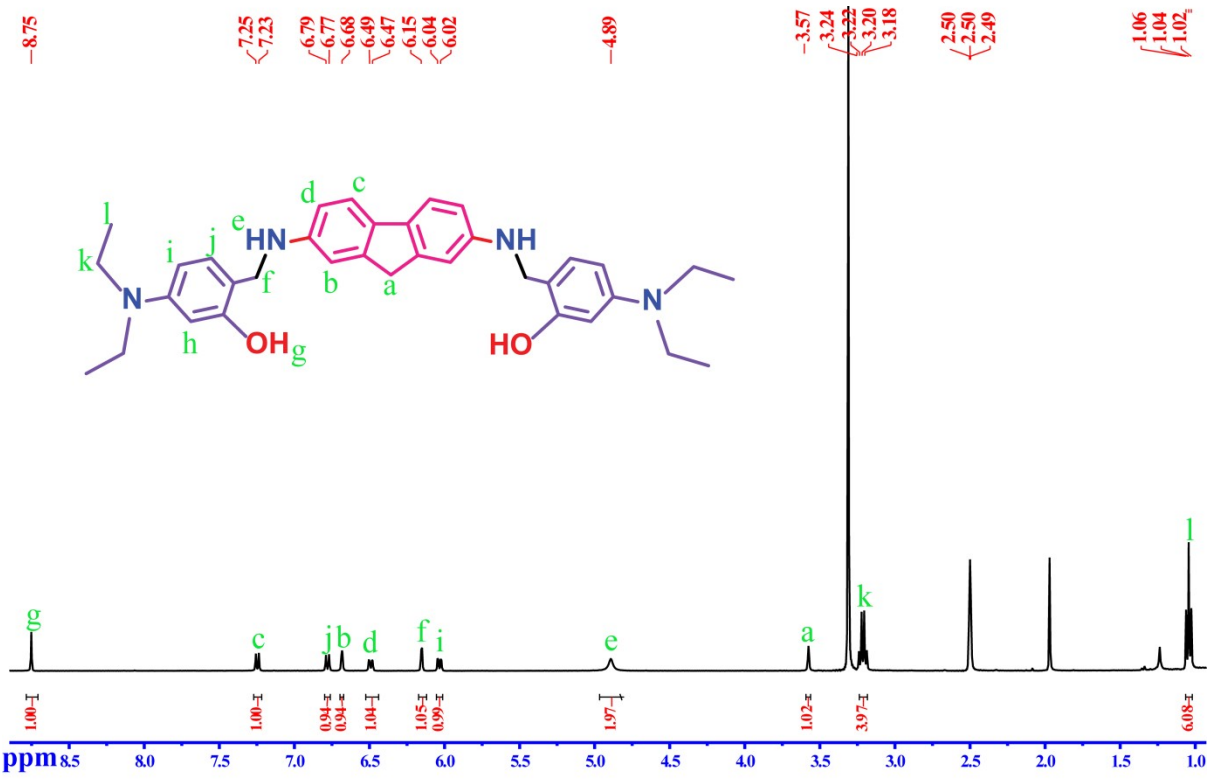

Figure S2: ^{1}H NMR of $\mathbf{L_1}$ in DMSO-d_6 at room temperature.

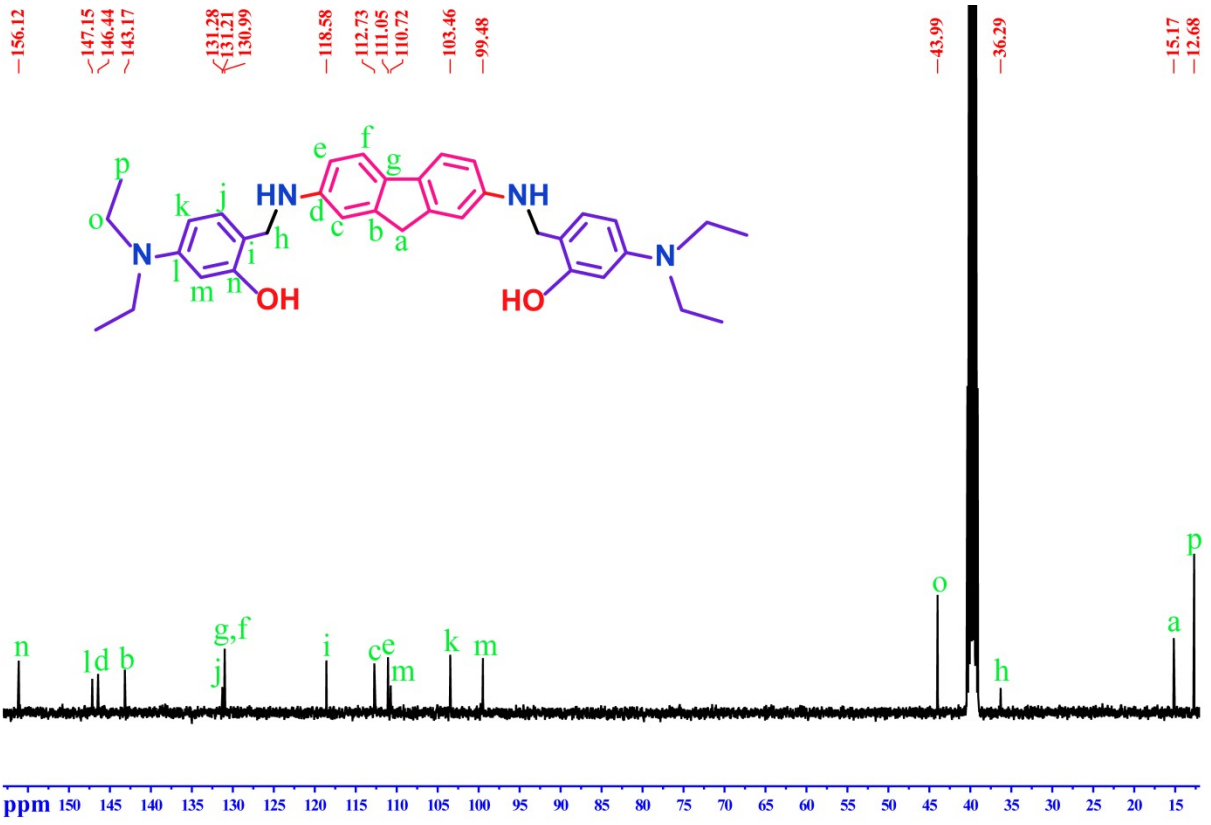

Figure S3: ^{13}C NMR of $\mathbf{L_1}$ in DMSO-d_6 at room temperature.

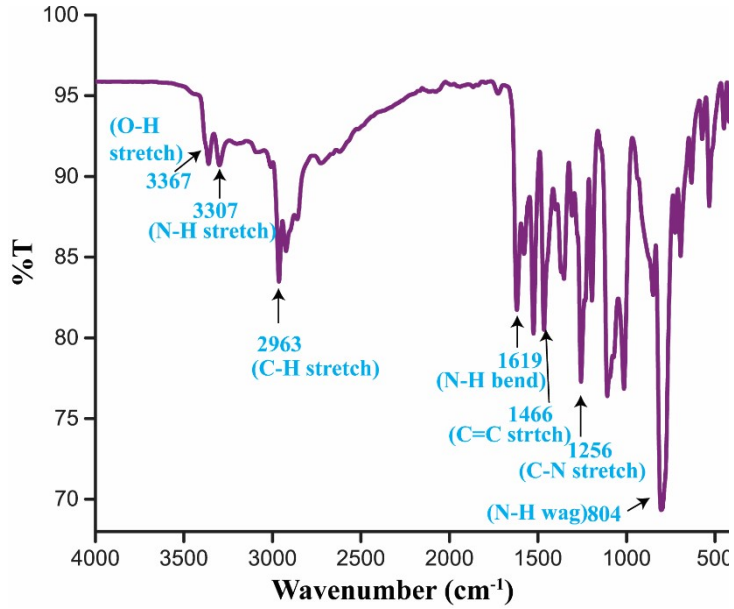

Figure S4: FTIR spectrum of $\mathbf{L_1}$ recorded in KBr pellet at room temperature.

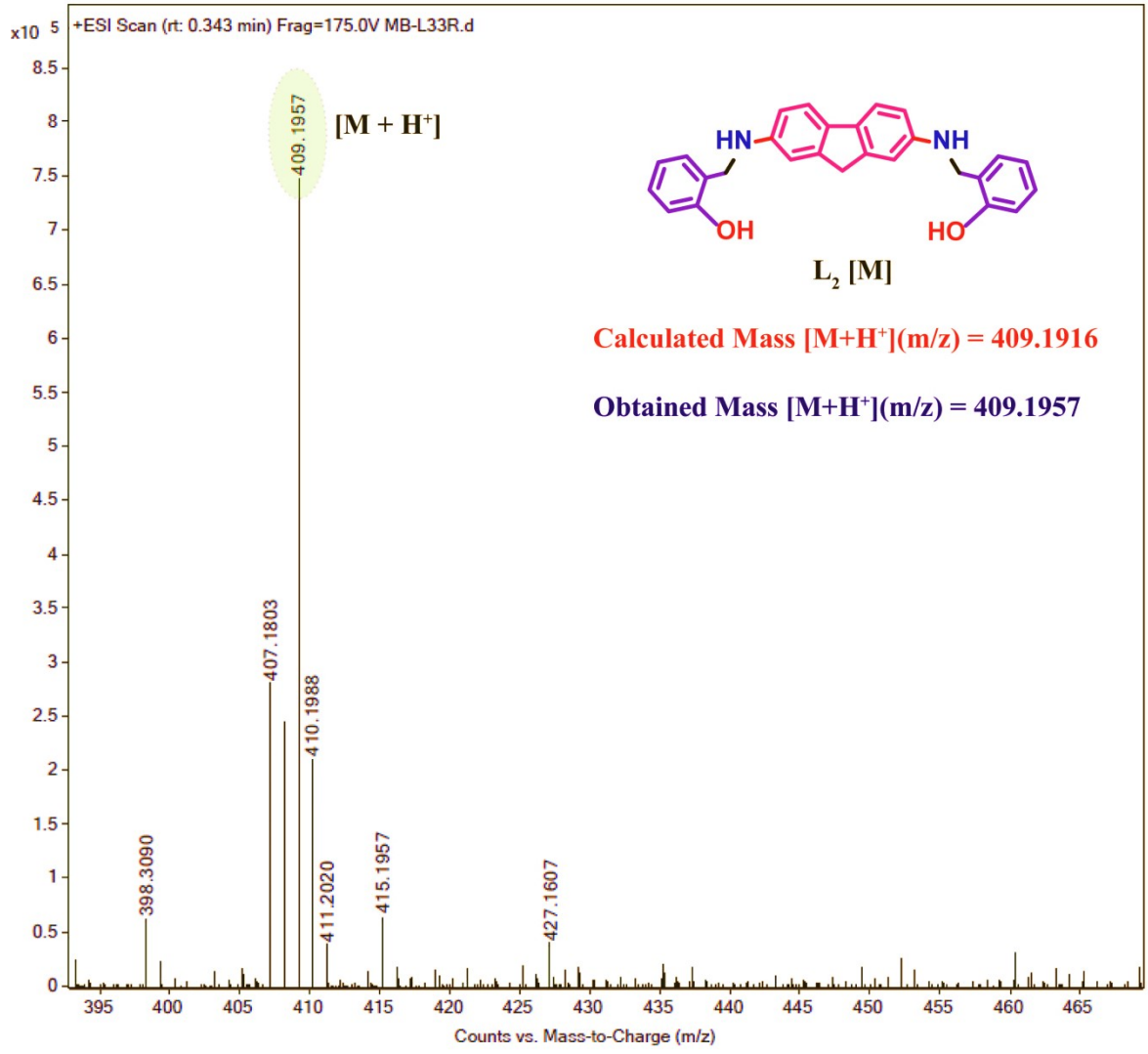

Figure S5: ESI-MS spectra of $\mathbf{L_2}$ in 1:1 water-acetonitrile in positive ionization mode.

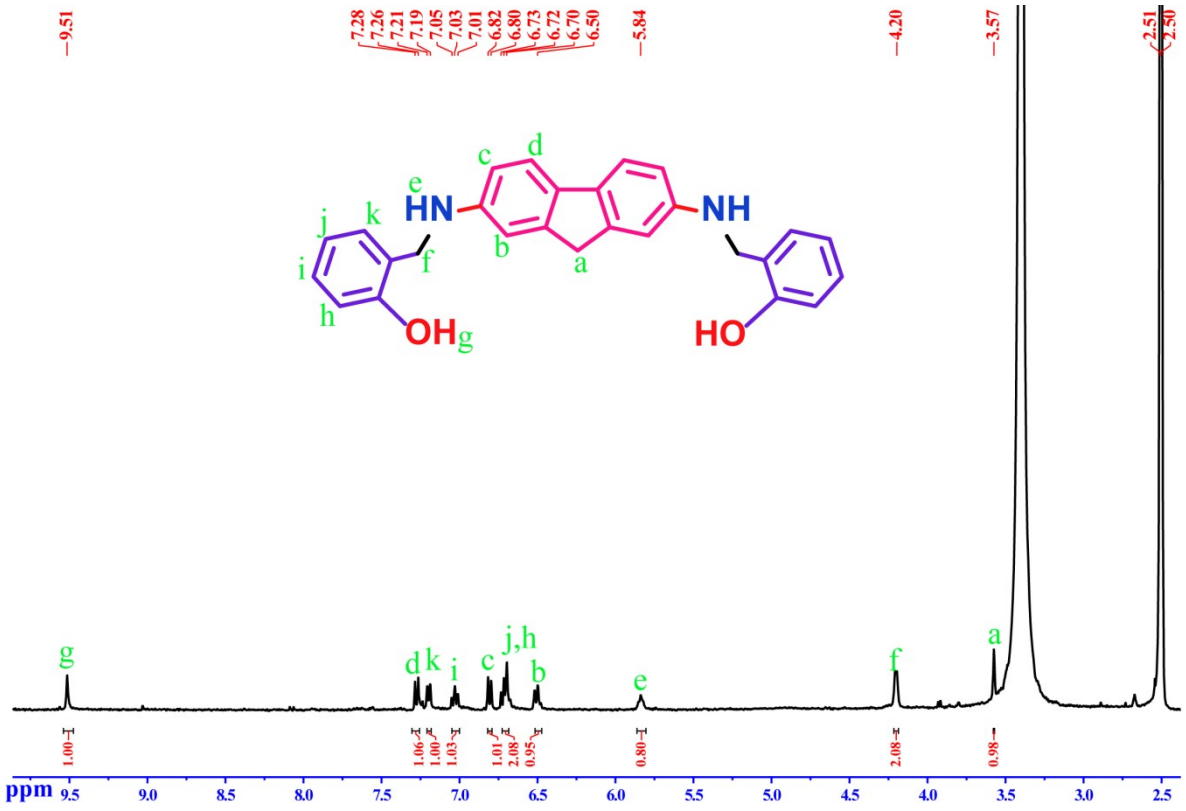

Figure S6: ^{1}H NMR of $\mathbf{L_2}$ in DMSO-d_6 at room temperature.

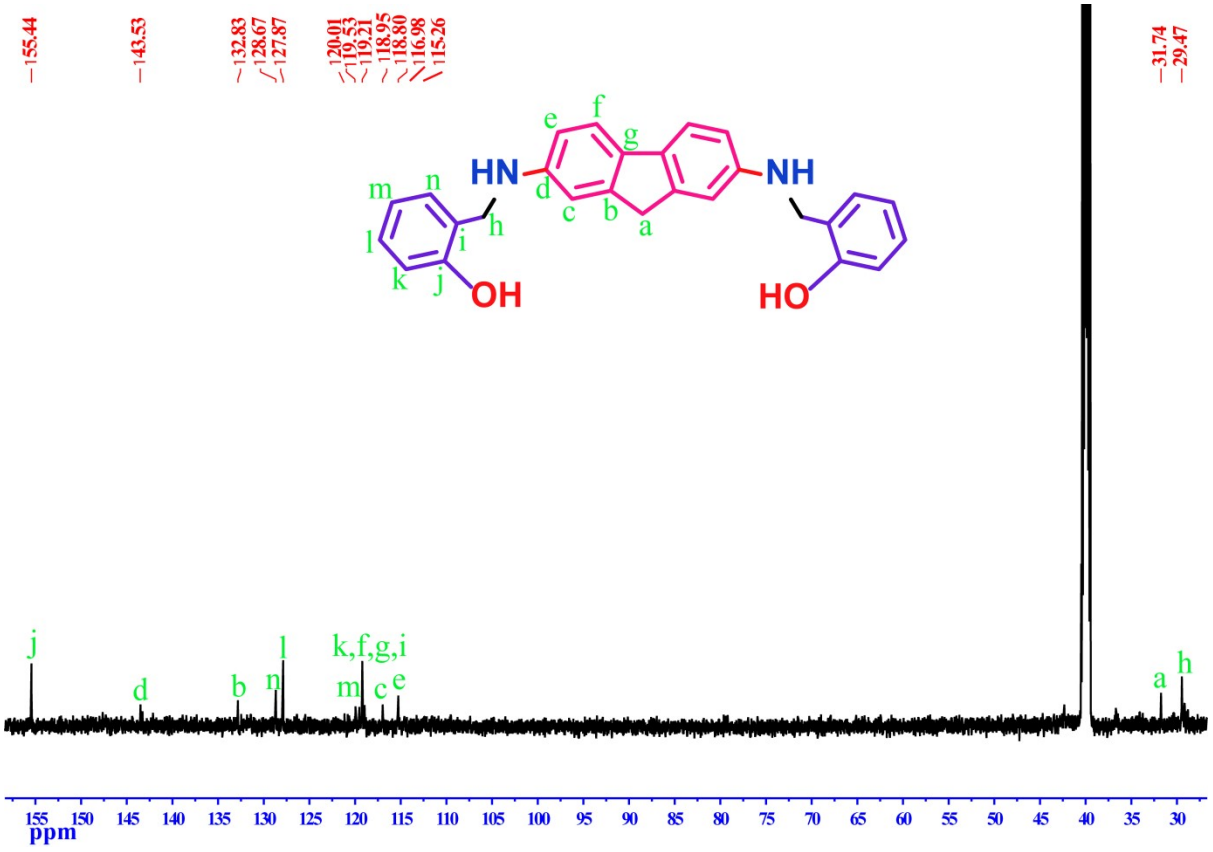

Figure S7: ^{13}C NMR of $\mathbf{L_2}$ in DMSO-d_6 at room temperature.

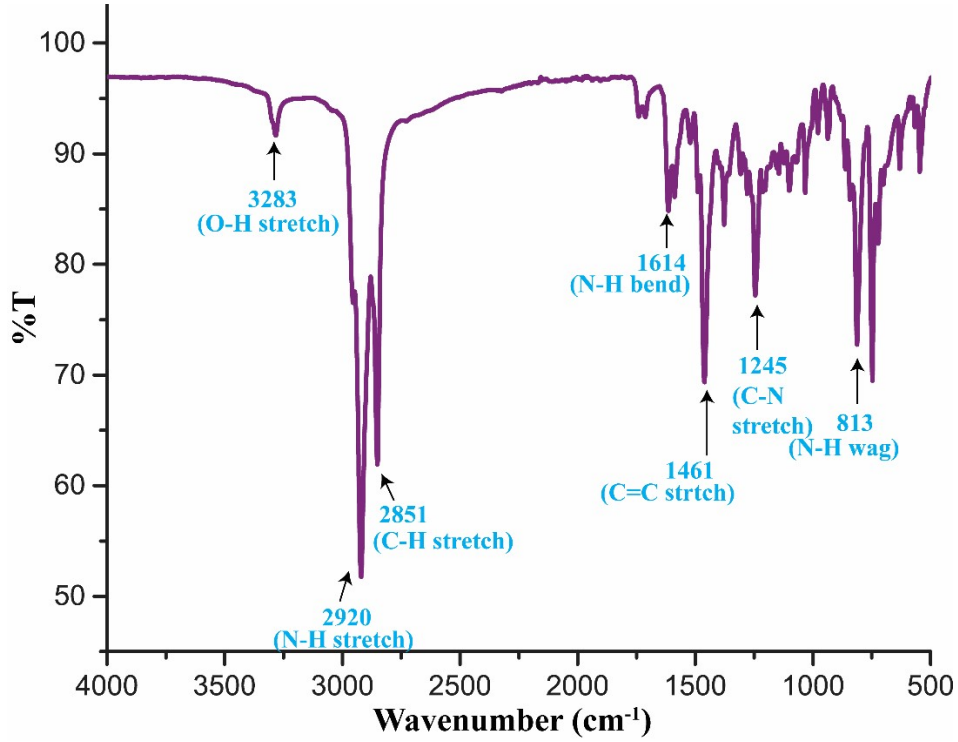

Figure S8: FTIR spectrum of $\mathbf{L_2}$ recorded in KBr pellet at room temperature.

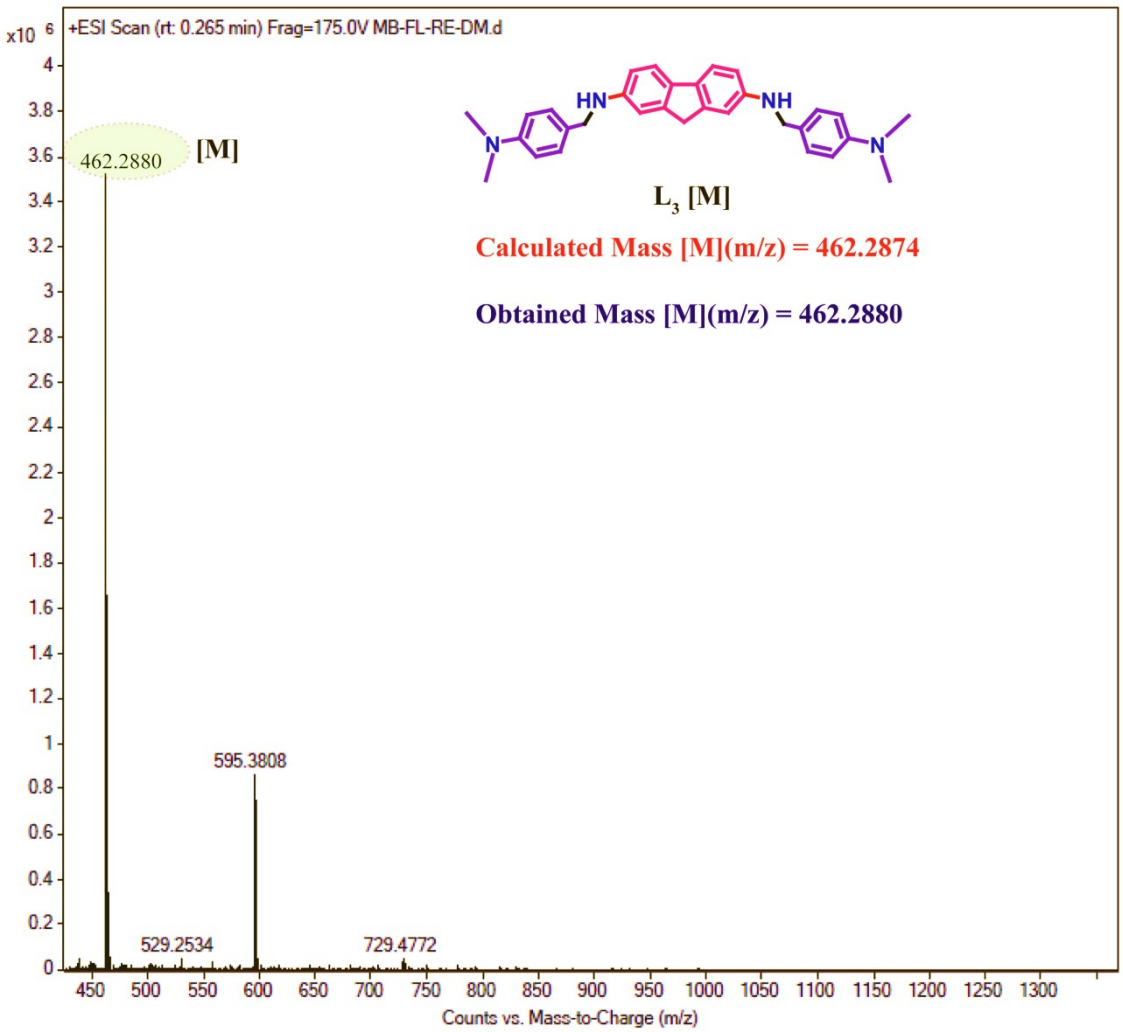

Figure S9: ESI-MS spectra of $\mathbf{L_3}$ in 1:1 water-acetonitrile in positive ionization mode.

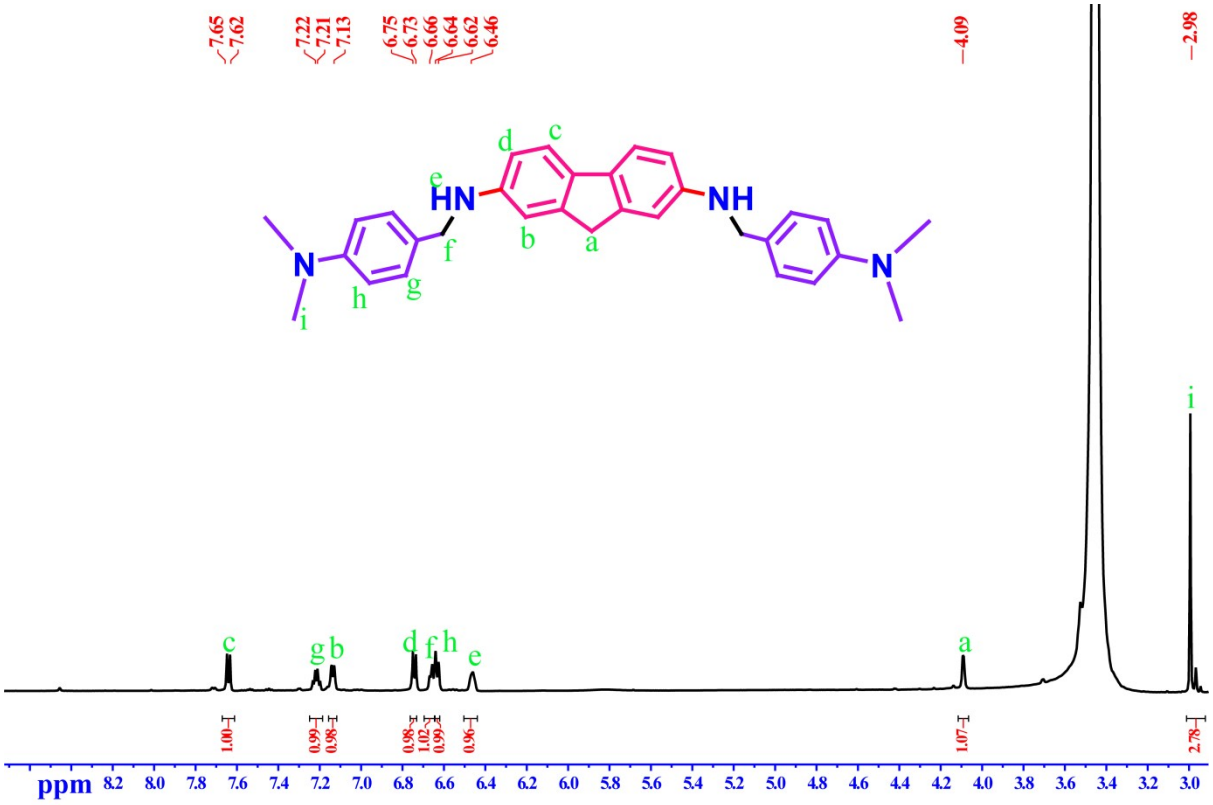

Figure S10: ^{1}H NMR of **L_3** in DMSO-d_6 at room temperature.

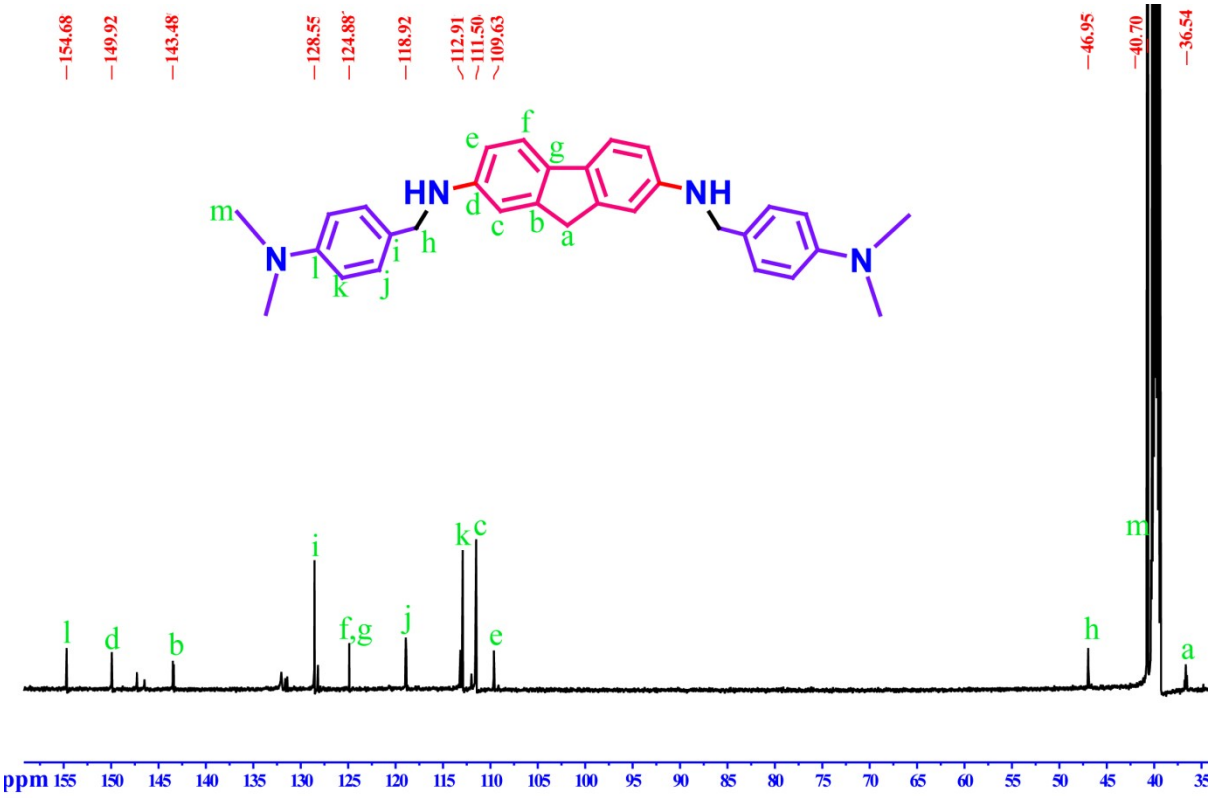

Figure S11: ^{13}C NMR of **L_3** in DMSO-d_6 at room temperature.

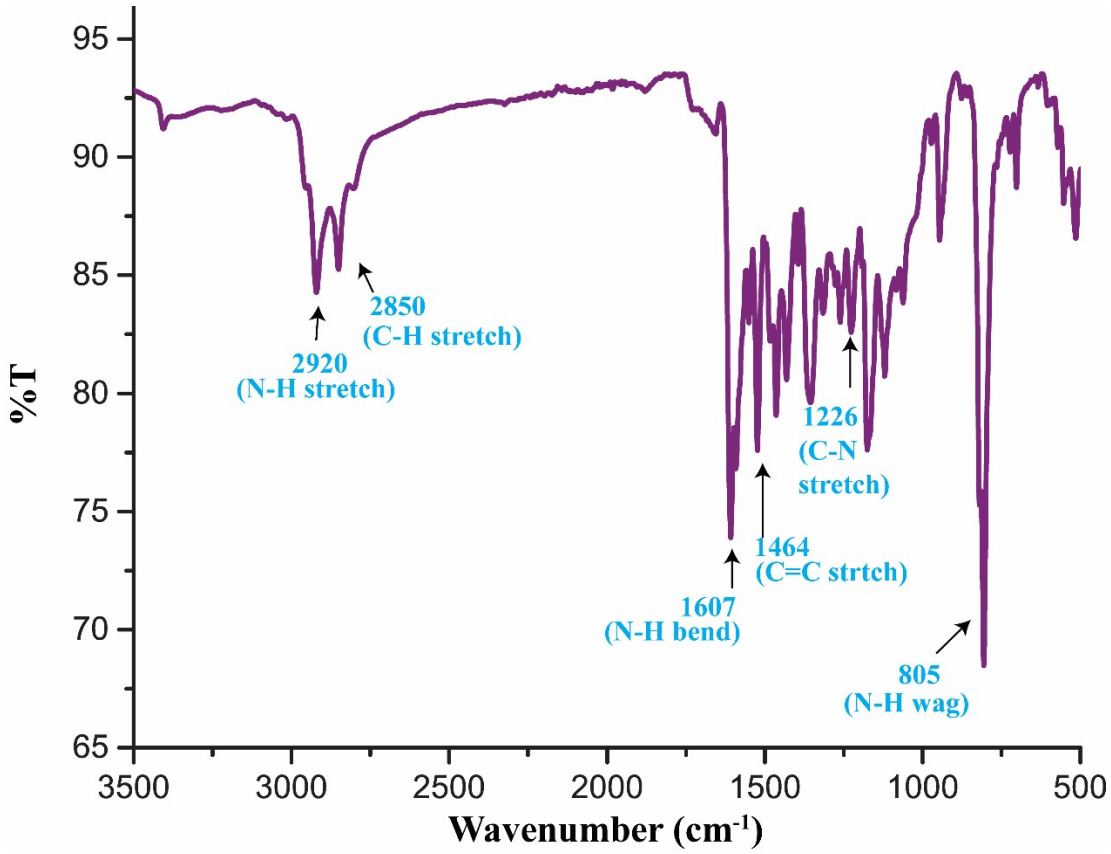

Figure S12: FTIR spectrum of $\mathbf{L_3}$ recorded in KBr pellet at room temperature.

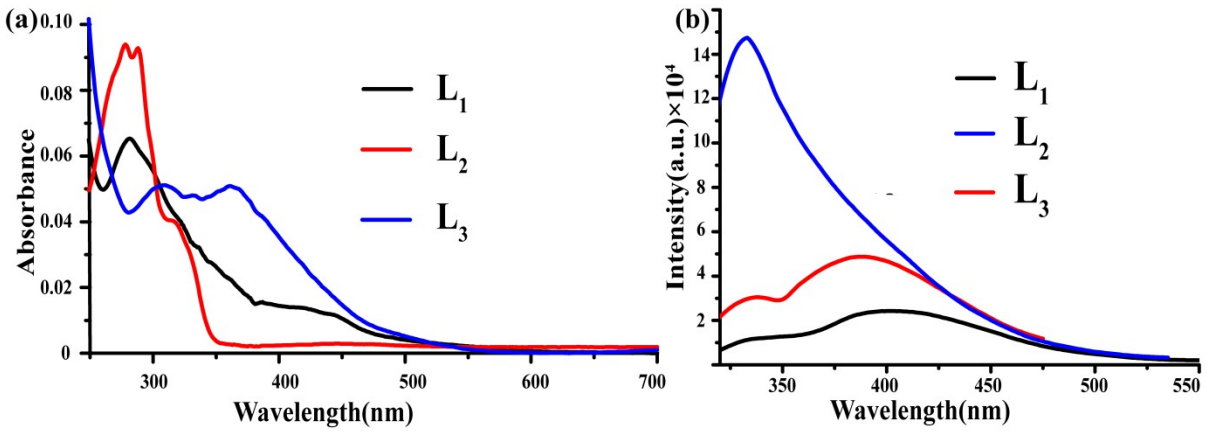

Figure S13: (a) UV-visible spectra of $\mathbf{L_1}$, $\mathbf{L_2}$ and $\mathbf{L_3}$ in aqueous medium at room temperature. (b) Fluorescence emission spectra of $\mathbf{L_1}$, $\mathbf{L_2}$ and $\mathbf{L_3}$ in aqueous medium at room temperature (λ_{ex} = 315 nm, slit = 3nm / 3nm).

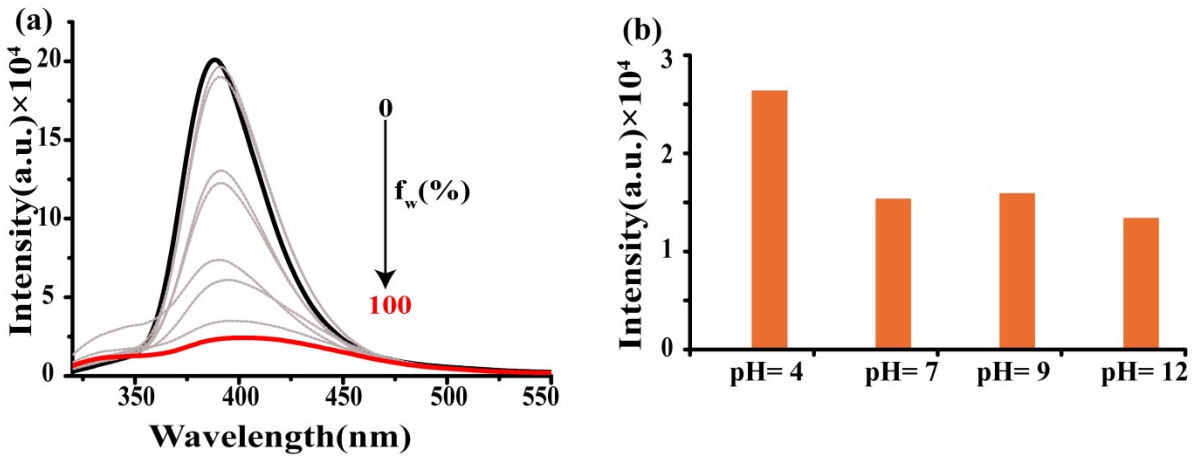

Figure S14: (a) Fluorescence spectral changes of $\mathbf{L_1}$ with increasing water content in acetonitrile solution (λ_{ex} = 315 nm, slit = 3nm / 3nm).(b) Fluorescence spectral changes of $\mathbf{L_1}$ with increasing pH in aqueous solution (λ_{ex} = 315 nm, slit = 3nm / 3nm).

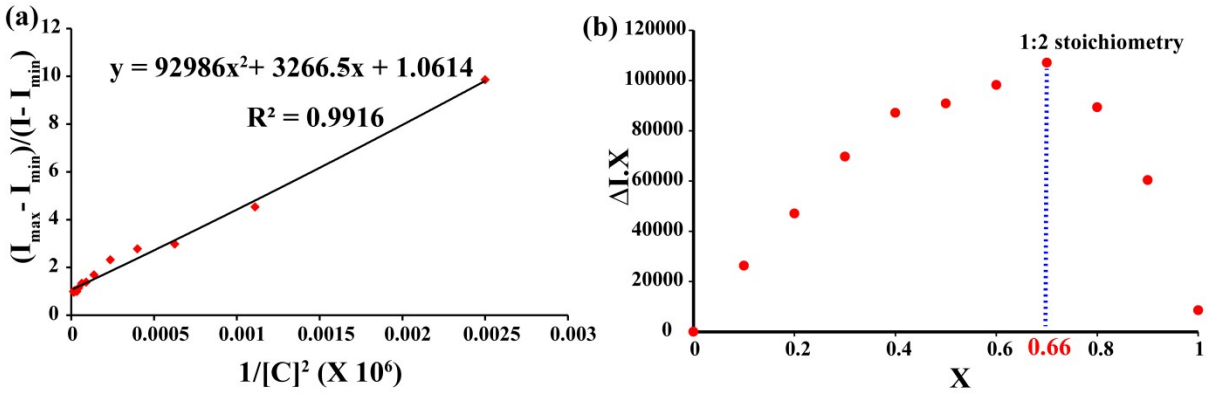

Figure S15: (a) Non-linear equation for titration of $\mathbf{L_1}$ with Hg^{2+} in aqueous medium. (b) Job's plot for determining $\mathbf{L_1}$'s stoichiometry with Hg^{2+} (1:2 host-guest complex).

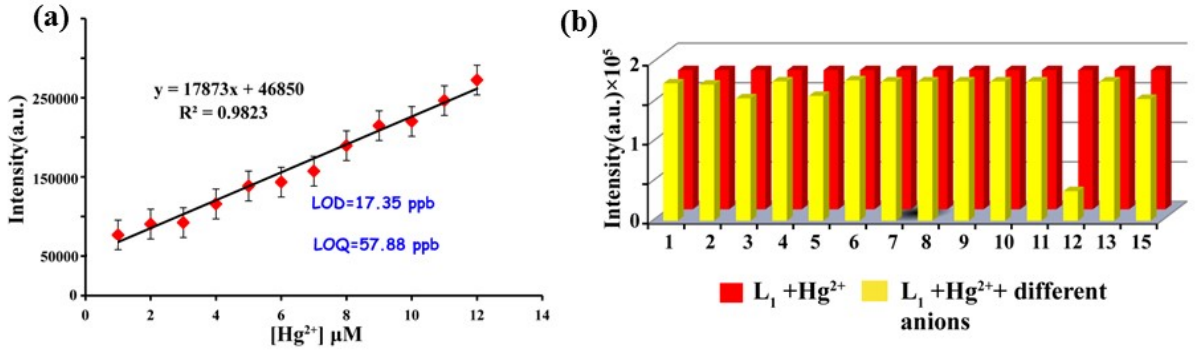

Figure S16: (a) Fluorescence emission intensity of $\mathbf{L_1}$ at 414 nm vs. Hg^{2+} concentration to calculate the limit of detection (LOD). (b) Fluorescence response of $\mathbf{L_1}$ (2.0 µM) to various analytes (1= Cl^-, 2= Br^-, 3= I^-, 4= F^-, 5= OH^-, 6= $H_2PO_4^-$, 7= SO_4^{2-}, 8=HSO_4^-, 9=cysteine, 10= homocysteine, 11= glutathione, 12= S^{2-} , 13= HSO_3^- and 14= NO_3^-).

Table S1: Fluorescence lifetime values of $\mathbf{L_1}$ (2.0 μM) and $\mathbf{L_1}$-Hg^{2+} in aqueous medium.

Sample	B_1	ΔB_1	B_2	ΔB_2	a_1	Δa_1	a_2	Δa_2	τ_1	$\Delta\tau_1$	τ_2	$\Delta\tau_2$	<τ> (ns)	χ^2
L_1	0.05	0.0005	0.02	0.0001	0.82	0.01	0.17	0.01	1.14	0.01	5.28	0.006	1.87	1.0
L_1+Hg^{2+}	0.03	0.0004	0.01	0.0002	0.27	0.07	0.73	0.07	1.42	0.02	6.85	0.008	5.37	1.0

Table S2: Rate constants for radiative and non-radiative decays, average lifetimes of $\mathbf{L_1}$ (2.0 μM) and $\mathbf{L_1}$-Hg^{2+} in aqueous medium.

Sample	K_r(S^{-1})	K_{nr}(S^{-1})	Slower decay component	Faster decay component	Average lifetime(ns)
$\mathbf{L_1}$	0.00069×10^9	0.53×10^9	1.14	5.28	1.87
$\mathbf{L_1}$ + Hg^{2+}	0.009×10^9	0.18×10^9	1.42	6.85	5.37

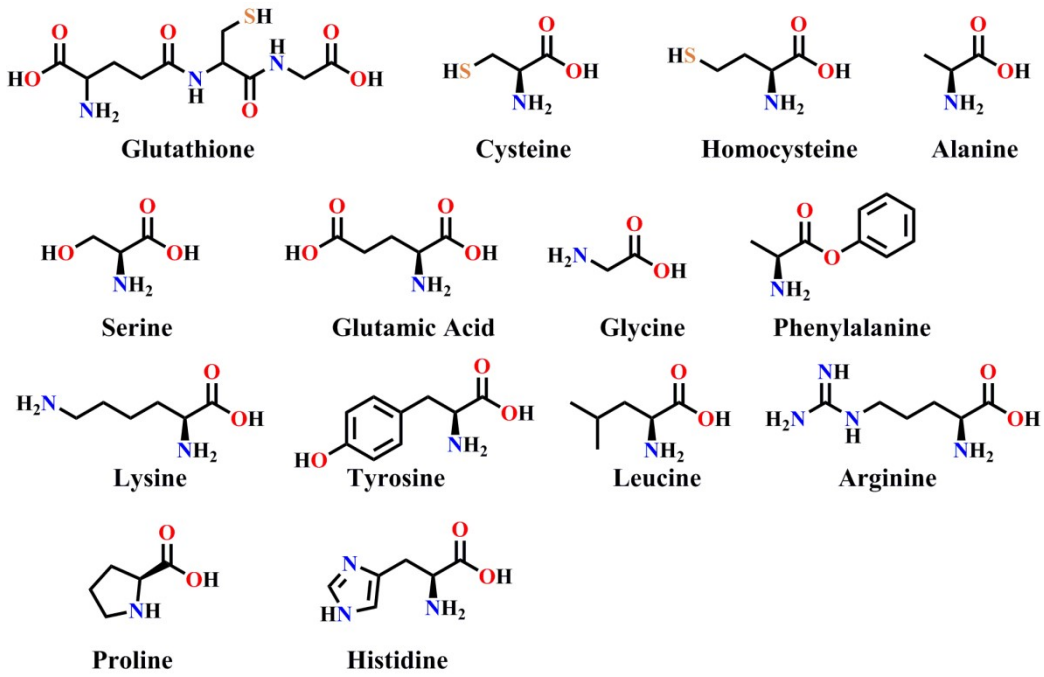

Figure S17: Chemical structures of different amino acids used in our study.

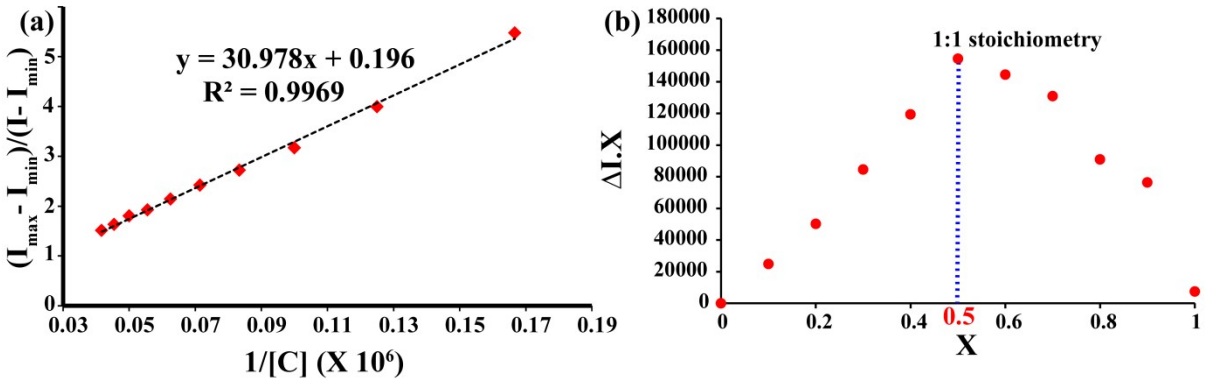

Figure S18: (a) Determination of affinity constant of $\mathbf{L_1}$ for GSH in aqueous medium using the Benesi-Hildebrand method. (b) Job's plot for determining $\mathbf{L_1}$'s stoichiometry with GSH (1:1 host-guest complex).

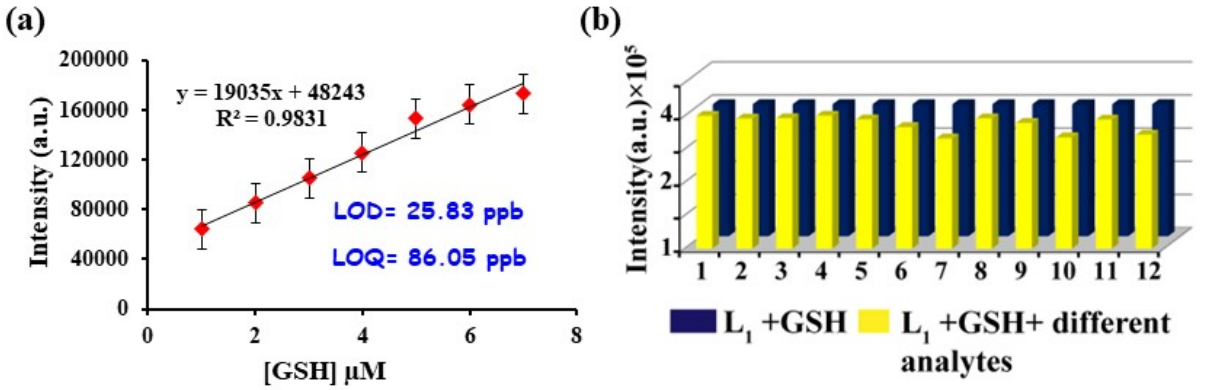

Figure S19: (a) Fluorescence emission intensity of $\mathbf{L_1}$ at 420 nm vs. GSH concentration to calculate the limit of detection (LOD). (b) Fluorescence response of $\mathbf{L_1}$ (2.0 µM) to various analytes (1=Cl^-, 2=Br^-, 3=I^-, 4=F^-, 5=NO_3^-, 6=$H_2PO_4^-$, 7=HCO_3^-, 8=HSO_4^-, 9=NO_2^-, 10= Hg^{2+}, 11=Cu^{2+} and 12=Zn^{2+})

Table S3: Fluorescence lifetime values of $\mathbf{L_1}$ (2.0 µM) and $\mathbf{L_1}$-GSH in aqueous medium.

Sample	B_1	ΔB_1	B_2	ΔB_2	a_1	Δa_1	a_2	Δa_2	τ_1	$\Delta\tau_1$	τ_2	$\Delta\tau_2$	$\langle\tau\rangle$ (ns)	χ^2
L_1	0.05	0.0005	0.02	0.0001	0.82	0.01	0.17	0.01	1.14	0.01	5.28	0.006	1.87	1.0
L_1+GSH	0.02	0.0017	0.02	0.0006	0.17	0.02	0.83	0.02	1.62	0.03	7.00	0.007	6.09	1.0

Table S4: Rate constants for radiative and non-radiative decays, average lifetimes of $\mathbf{L_1}$ (2.0 μM) and $\mathbf{L_1}$-GSH in aqueous medium.

Sample	K_r(S^{-1})	K_{nr}(S^{-1})	Slower decay component	Faster decay component	Average lifetime(ns)
$\mathbf{L_1}$	0.00069×10^9	0.53×10^9	1.14	5.28	1.87
$\mathbf{L_1}$ + GSH	0.07×10^9	0.09×10^9	1.62	7.0	6.09

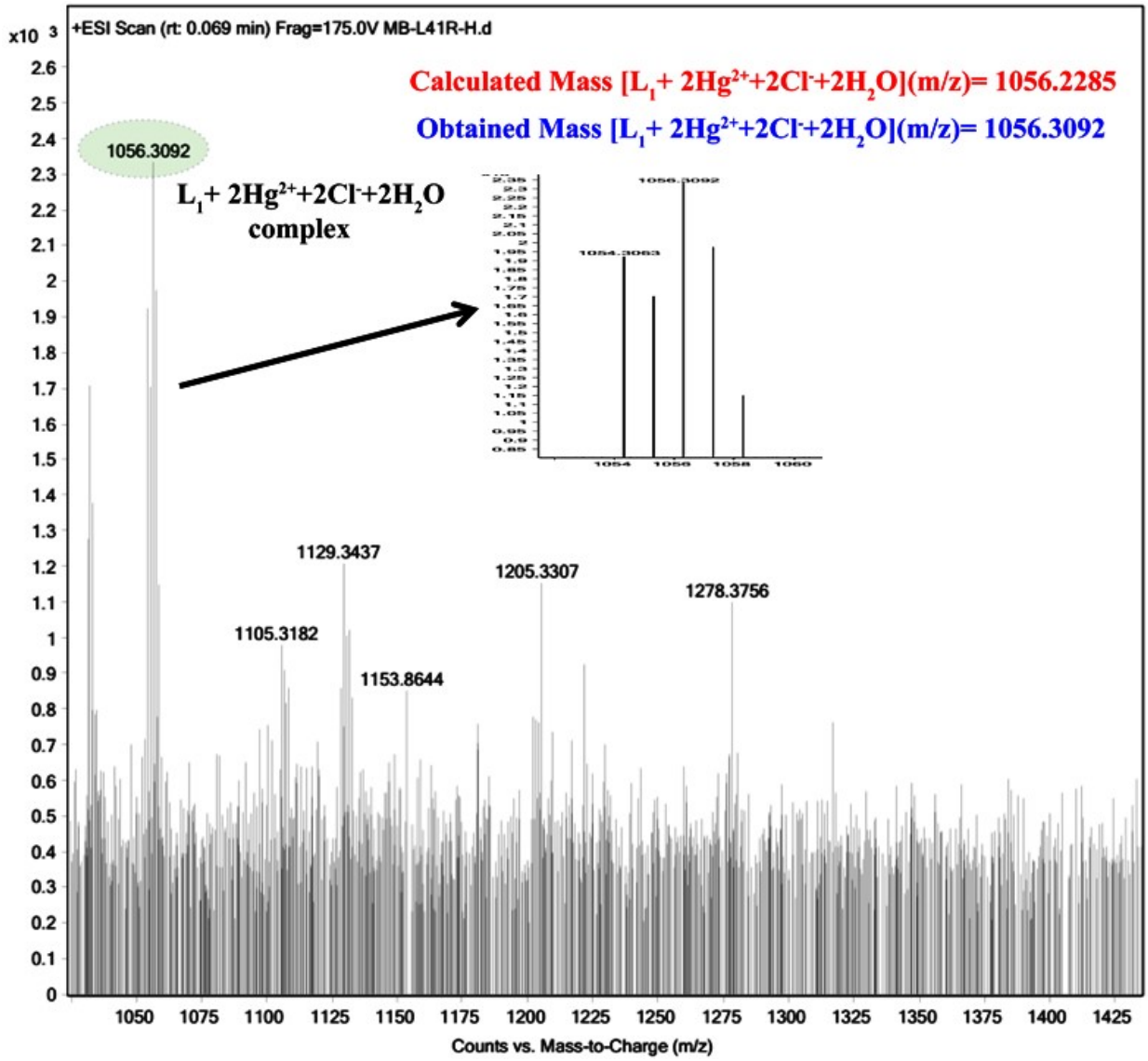

Figure S20: ESI-MS spectra of $\mathbf{L_1}$ in 1:1 water-acetonitrile in the presence of Hg^{2+} in positive ionization mode.

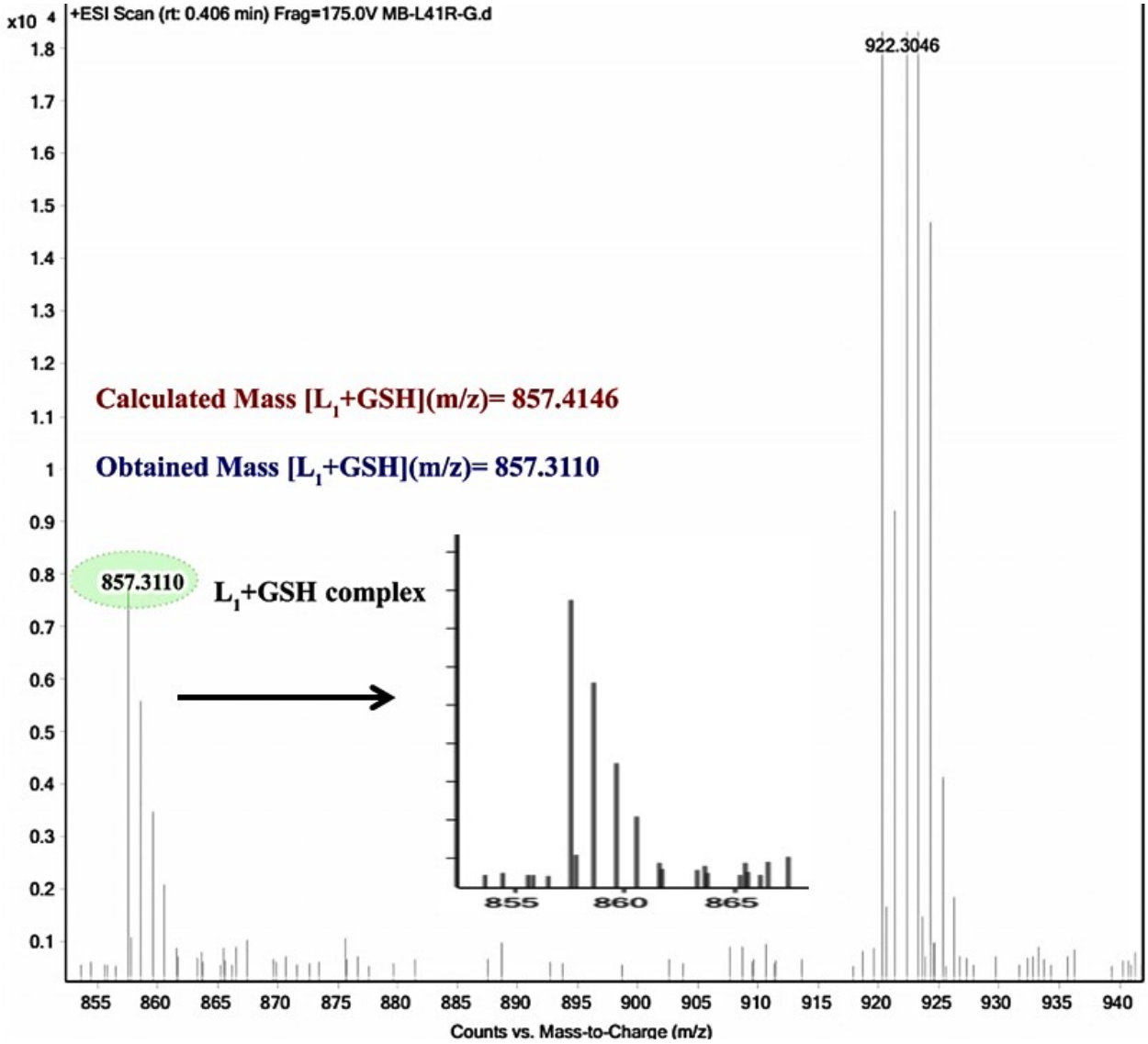

Figure S21: ESI-MS spectra of $\mathbf{L_1}$ in 1:1 water-acetonitrile in the presence of GSH in positive ionization mode.

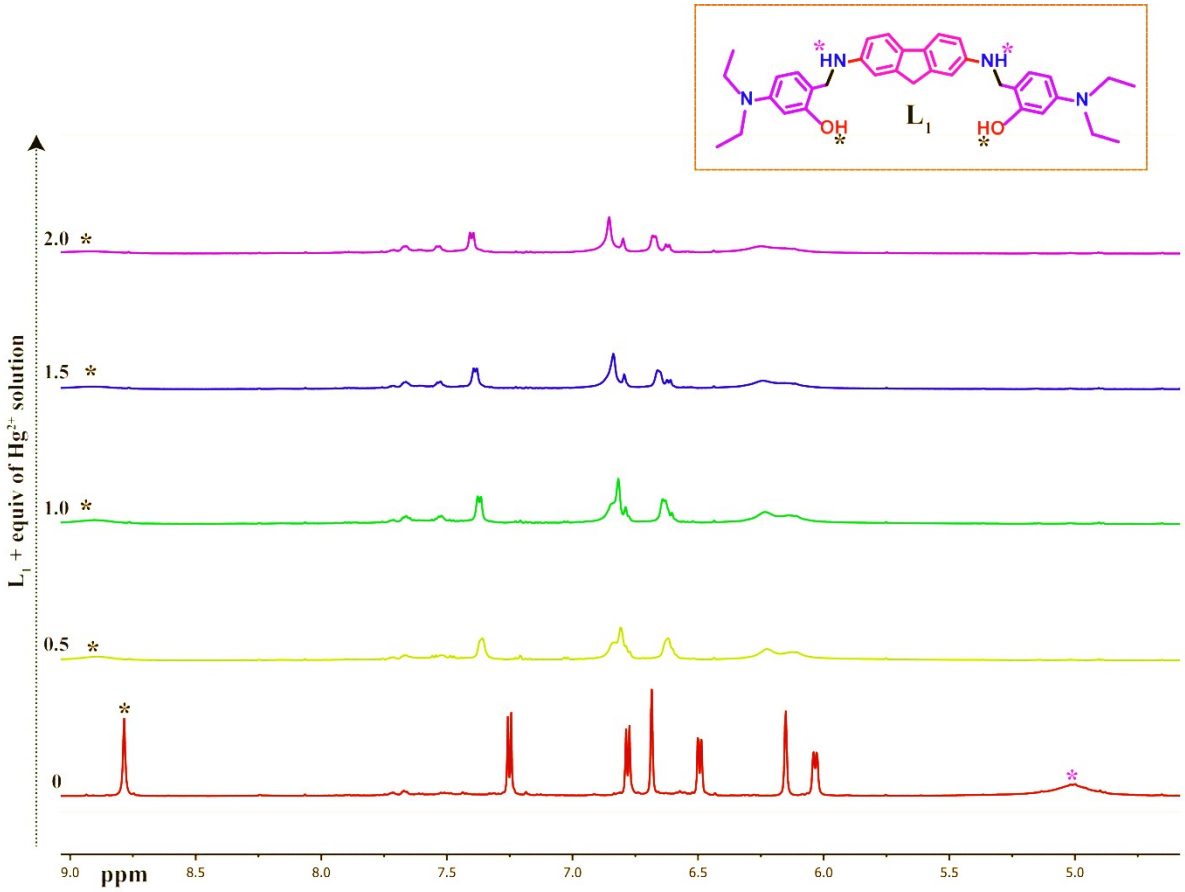

Figure S22: ^{1}H NMR spectral changes of $\mathbf{L_1}$ in DMSO-d_6 upon titration with 2 equiv.Hg^{2+} solution.

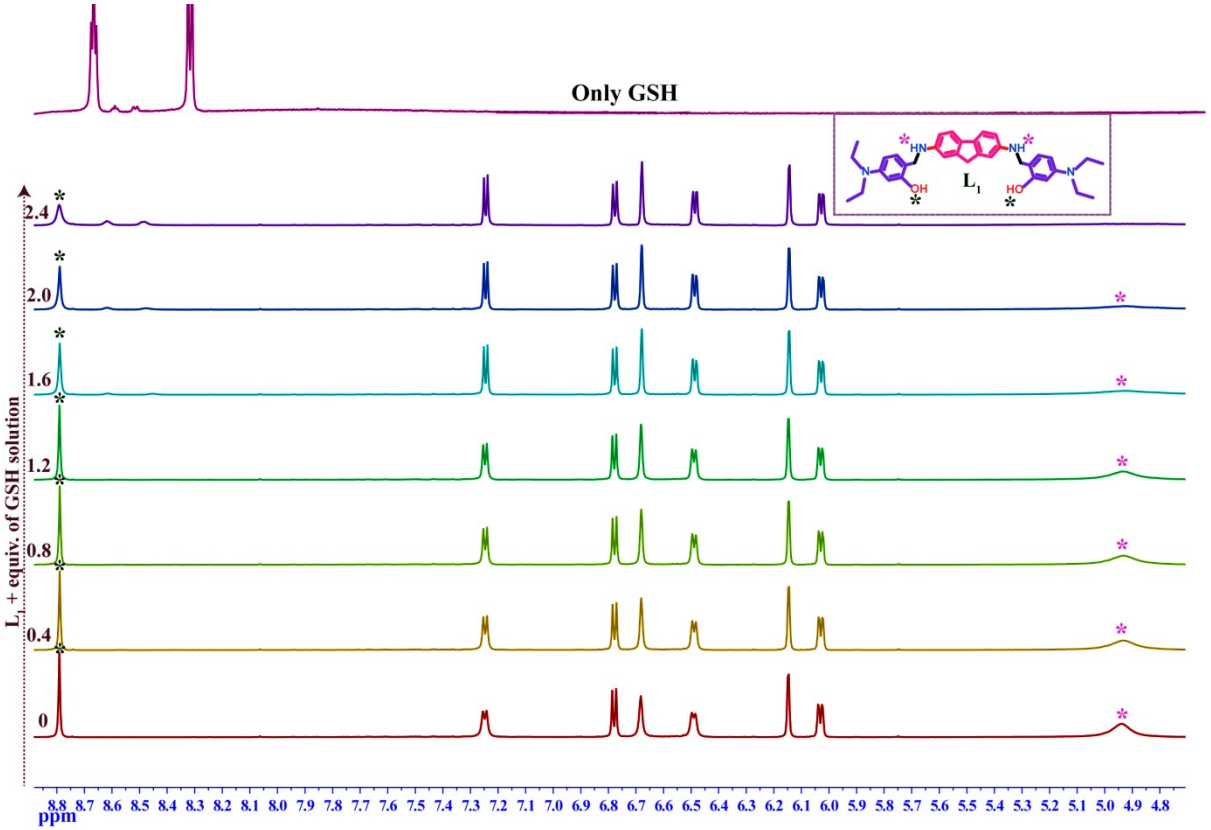

Figure S23: ^{1}H NMR spectral changes of $\mathbf{L_1}$ in DMSO-d_6 upon titration with 2.4 equiv. of GSH solution.

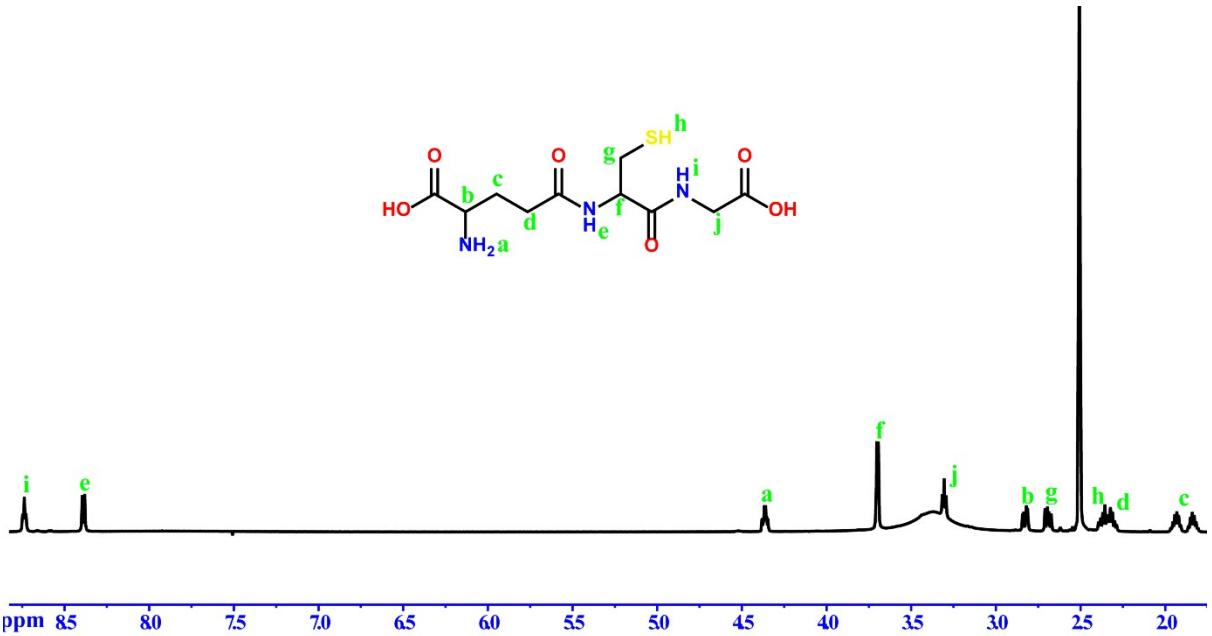

Figure S24: ^{1}H NMR spectral changes of **GSH** in DMSO-d_6.

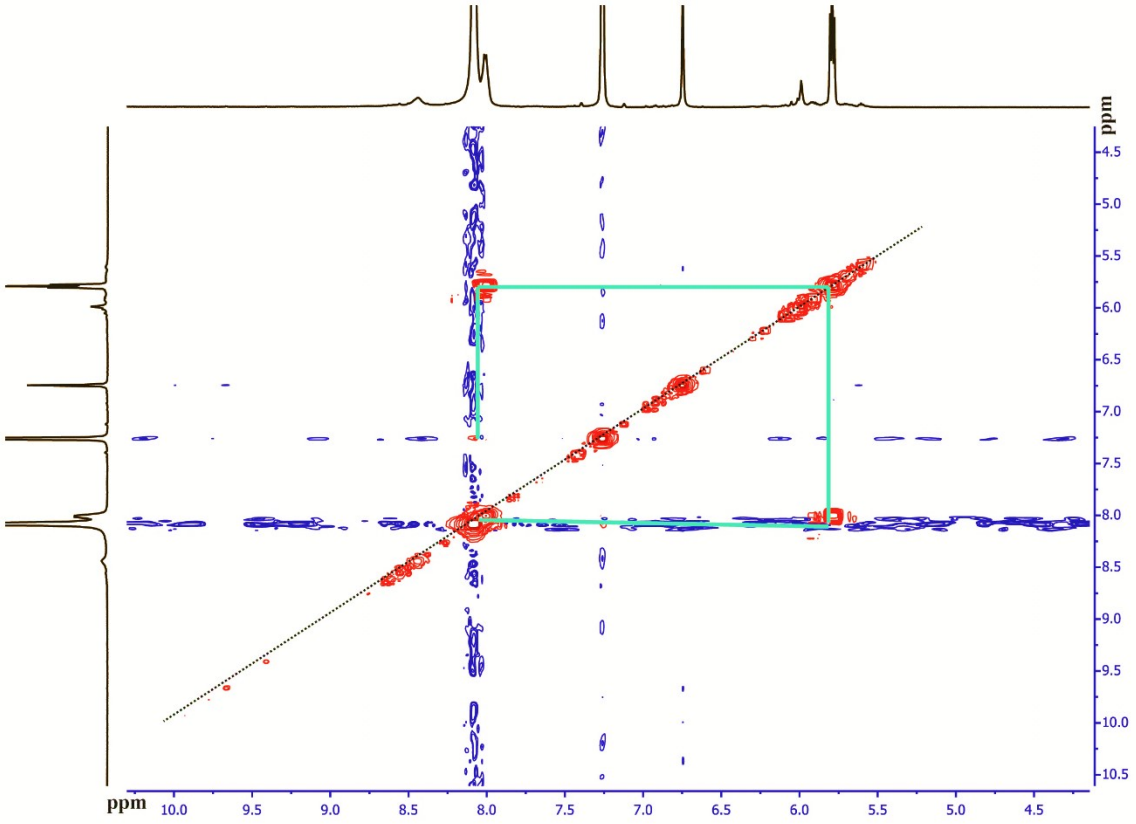

Figure S25: 2D ^{1}H-^{1}H COSY NMR spectra of $\mathbf{L_1}$- Hg^{2+} DMSO-d_6 (1:1 equiv).

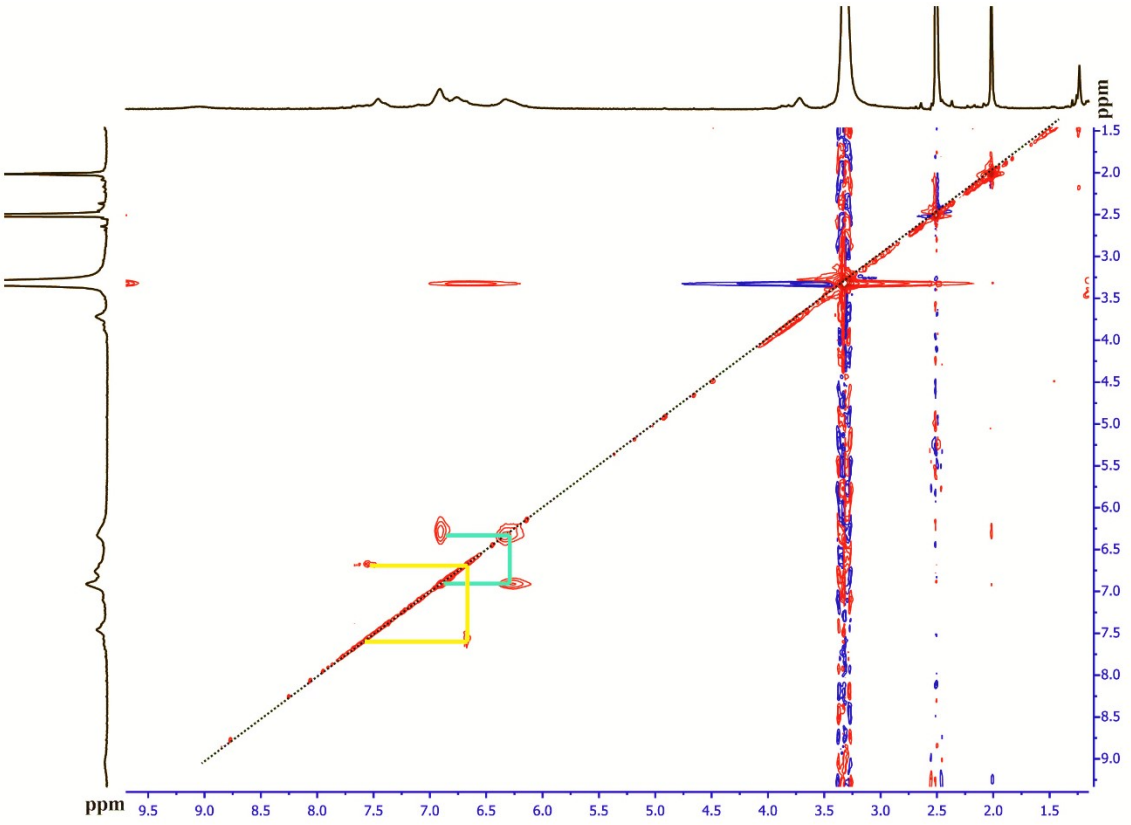

Figure S26: 2D ^{1}H-^{1}H TOCSY NMR spectra of $\mathbf{L_1}$- Hg^{2+} DMSO-d_6 (1:1 equiv).

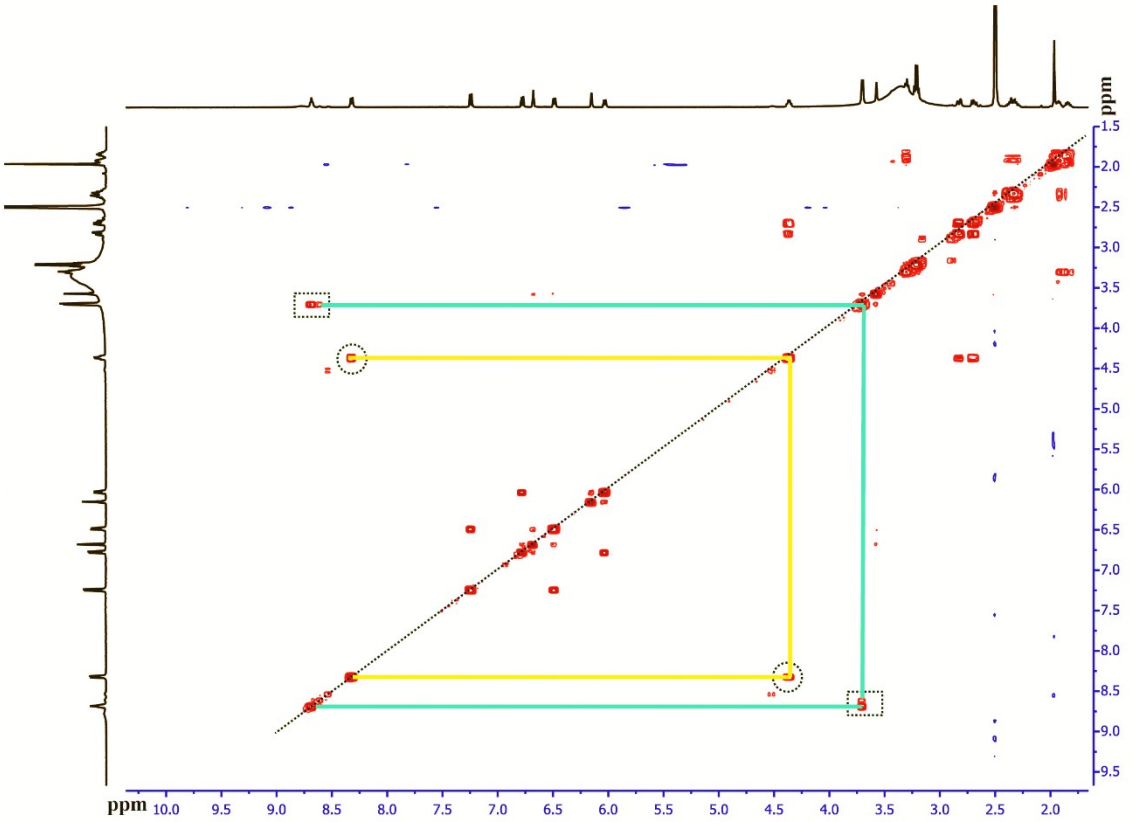

Figure S27: 2D ^{1}H-^{1}H COSY NMR spectra of **L_1**- GSH in DMSO-d_6 (1:1 equiv).

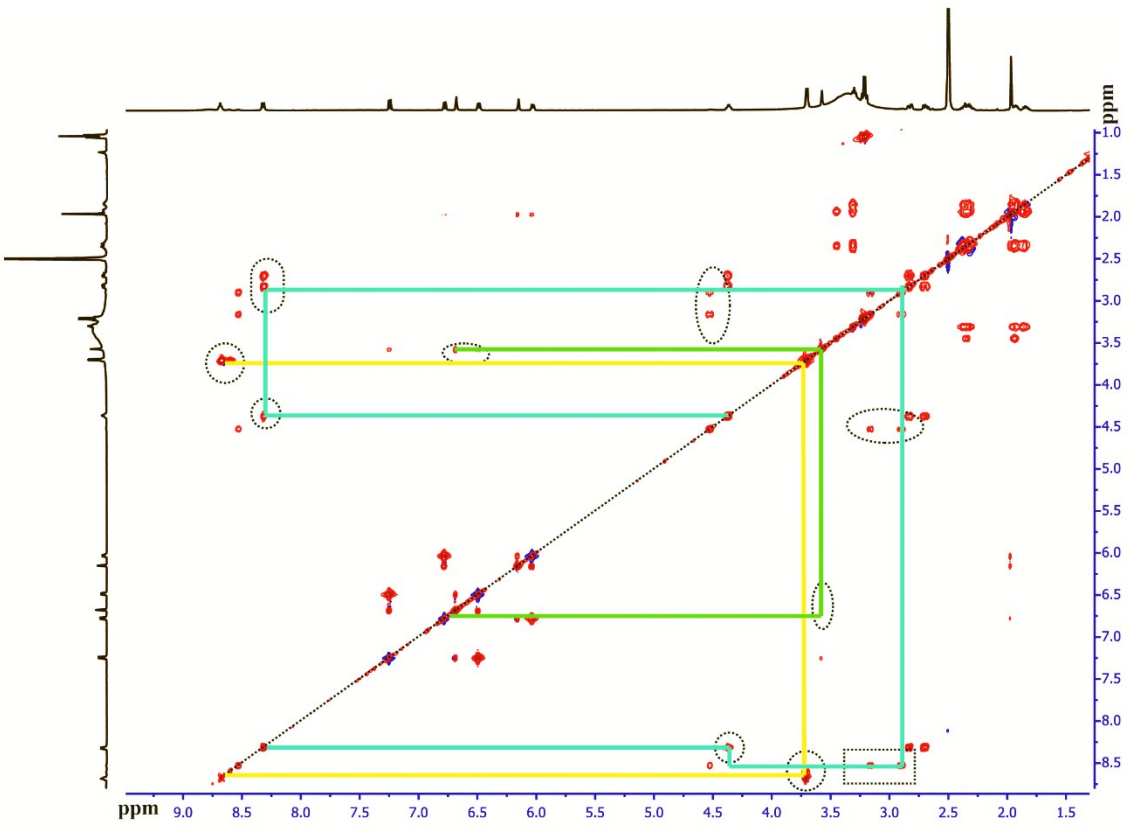

Figure S28: 2D ^{1}H-^{1}H TOCSY NMR spectra of **L_1**- GSH in DMSO-d_6 (1:1 equiv).

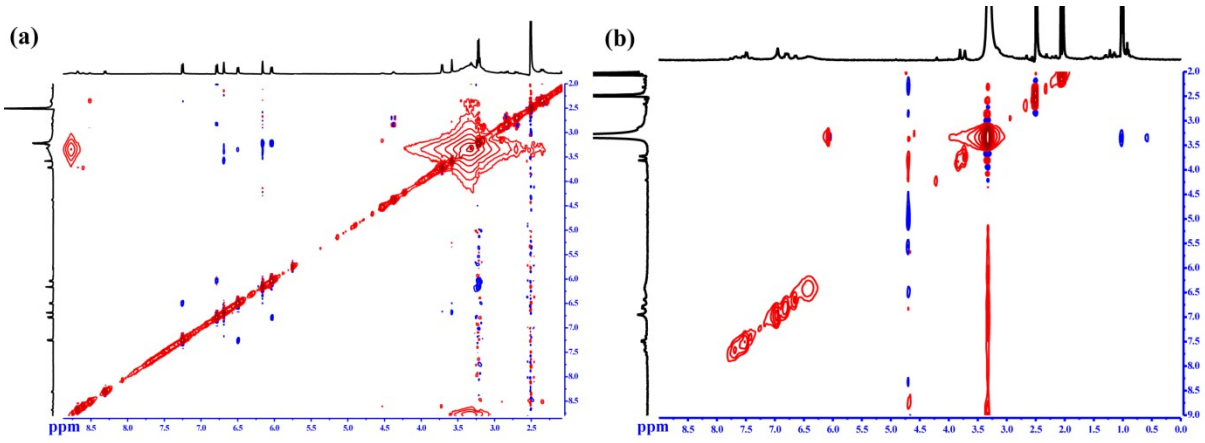

Figure S29: 2D-NOESY NMR spectra of $\mathbf{L_1}$ in presence of (a) GSH and (b) Hg^{2+}.

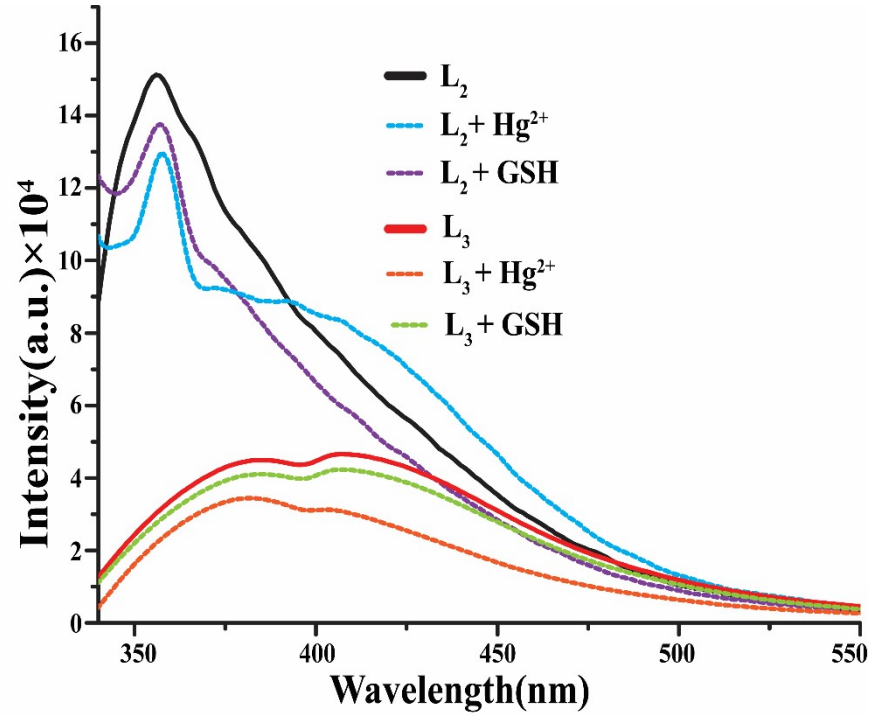

Figure S30: Fluorescence response of $\mathbf{L_2}$ and $\mathbf{L_3}$ towards Hg^{2+}/GSH.

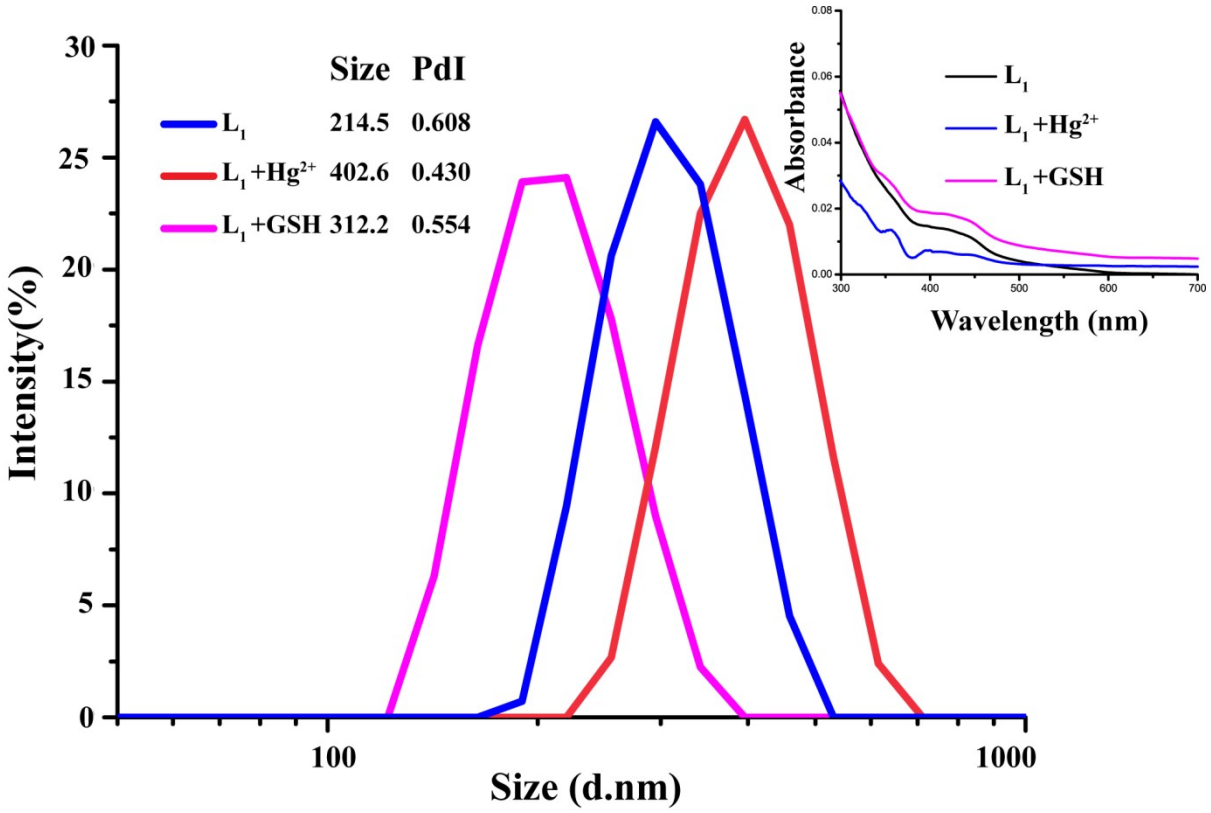

Figure S31: DLS analysis of $\mathbf{L_1}$ (2.0 μM) , $\mathbf{L_1}$ + Hg^{2+} and $\mathbf{L_1}$ + GSH in aqueous medium.(Inset: UV spectra of $\mathbf{L_1}$ + Hg^{2+} and $\mathbf{L_1}$ + GSH showing upliftment of baseline indication aggregation nature).

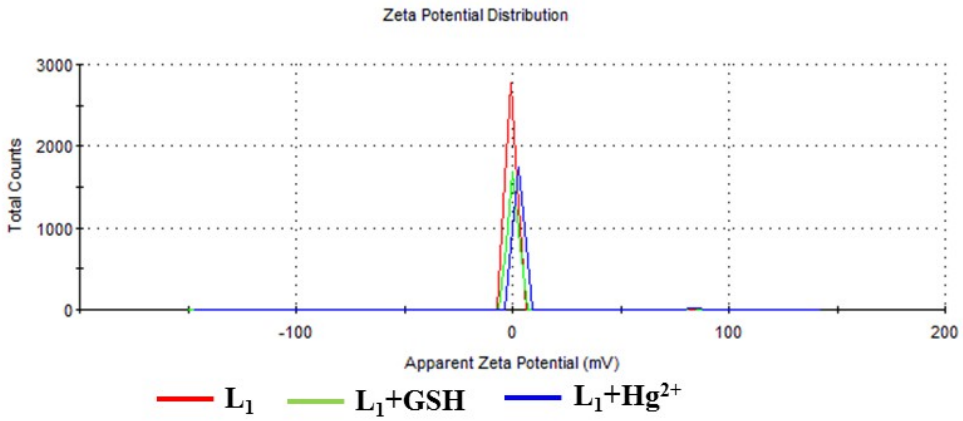

Figure S32: Zeta potential distribution of $\mathbf{L_1}$ in aqueous medium (pH = 7.4) before and after addition of analytes.

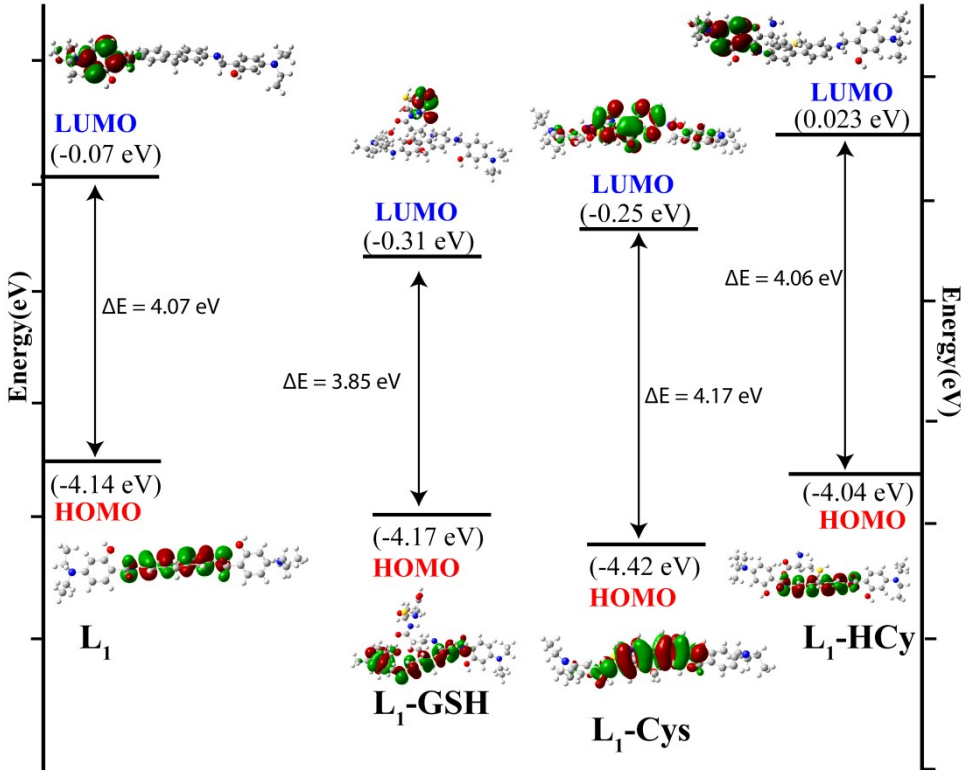

Figure S33: Comparative energy level diagrams of L_1 -cysteine ensemble; L_1 -homocysteine ensemble; L_1 -glutathione ensemble.

Table S5: Comparative analysis of Hg^{2+} in different real environmental samples by using fluorimetric method and AAS technique.

Sample	Fluoresceence Spectroscopy				Atomic Absorption Spectroscopy(AAS)			
	Added (µM)	Detected (µM)	Recovery (%)	RSD(%)n=3	Added (µM)	Detected (µM)	Recovery (%)	RSD(%)n=3
Drinking water	2.0	1.8	90	0.4	2.0	2.0	100	0.38
Tap water	2.0	1.9	94	1.35	2.0	1.95	97.5	1.4
Lake water	2.0	2.1	101	0.36	2.0	2.13	106	0.4
River water	2.0	1.85	93	2.35	2.0	1.8	90	2.20
Sea water	2.0	2.1	105	0.45	2.0	2.15	107	0.37
Industrial wastewater	2.0	2.25	110	3.26	2.0	2.24	112	3.00

Table S6: Determination of GSH in different real biological samples by using fluorimetric method and HPLC technique.

	Fluoresceence Spectroscopy				High-performance Liquid Chromatography(HPLC)			
Sample	**Added (μM)**	**Detected (μM)**	**Recovery (%)**	**RSD(%) n=3**	**Added (μM)**	**Detected (μM)**	**Recovery (%)**	**RSD (%)n =3**
White grape	2.0	1.85	92.5	0.28	2.0	1.7	87.5	0.58
Tomato	2.0	2.1	105	3.52	2.0	1.9	95	4.0
Watermelon	2.0	2.2	110	1.95	2.0	1.9	94	2.5
1:10 Diluted Human serum	2.0	2.1	104	0.32	2.0	1.8	90	0.52

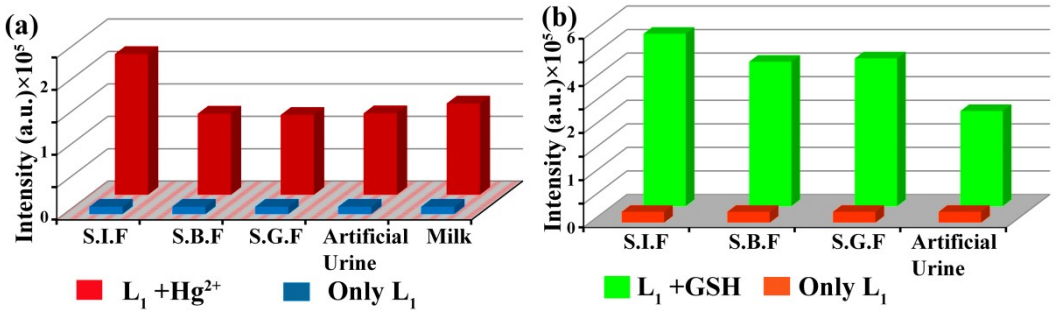

Figure S34: (a) Changes in the emission intensity of **L_1** (2.0 μM) at 414 nm in the presence of excess Hg^{2+} in simulated fluid samples [S.B.F- Simulated Body Fluid (pH~7.4), S.G.F- Simulated Gastric Fluid (pH~2.0) and S.I.F- Simulated Intestinal Fluid (pH~8.0)], artificial urine sample and milk sample.(b) Fluorescence response of **L_1** (2.0 μM) at 420 nm in the presence of excess GSH in simulated fluid samples [S.B.F- Simulated Body Fluid (pH~7.4), S.G.F- Simulated Gastric Fluid (pH~2.0) and S.I.F- Simulated Intestinal Fluid (pH~8.0)] and artificial urine sample.

Figure S35: RGB analysis by the color recogniser app.

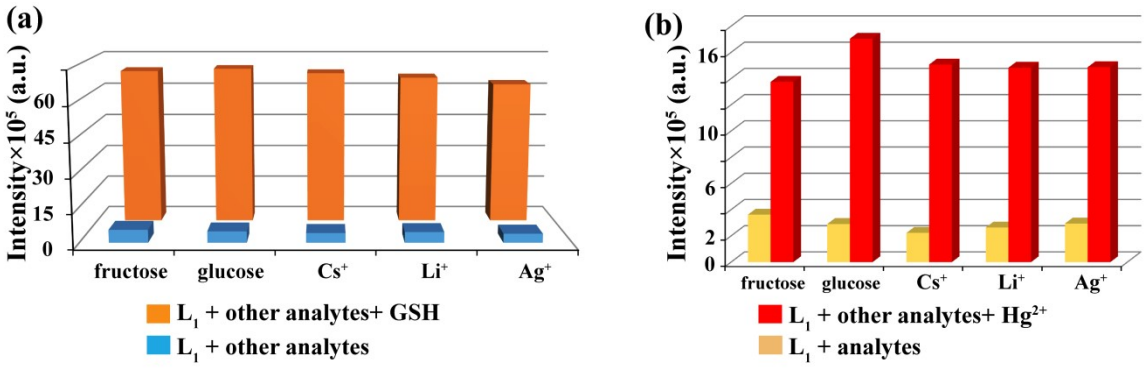

Figure S36:(a) Fluorescence response of $\mathbf{L_1}$ (2.0 μM) to various analytes in presence of GSH. (b) Fluorescence response of $\mathbf{L_1}$ (2.0 μM) to various analytes in presence of Hg^{2+}.

Table S7: A comparative study of the proposed receptor with some previously reported ones.

Sl No.	References	Receptor (Operation mode)	Solvent System	LOD(ppb)	Sensing analyte
1.	**Present work (Bifunctional receptor i.e. both for mercury(II) and GSH**	**Fluorene derivative (Off-on)**	**100% Aqueous medium**	**17.35 (0.0865 μM) 25.83 (0.0840 μM)**	**Hg^{2+} and GSH discretely**
2.	Spectrochimica Acta Part A: Molecular and Biomolecular Spectroscopy,2021, 257, 119316	Naphthoquinone probe (Off-on)	DMSO-H_2O (9:1, v/v) solution	90.46 (0.451 μM)	Hg^{2+}
3.	Spectrochimica Acta Part A: Molecular and Biomolecular Spectroscopy,2021, 250, 119776	Cytidine-Au nanoclusters (Colorimetric color change)	-	3073.2 (10 μM)	GSH, GSSH, GR
4.	Sensors and Actuators: B. Chemical., 2018, 255(Part1),657-665	Au/N-CQDs (On-off)	Aqueous medium	23.66 (0.118 μM)	Hg^{2+}
5.	Microchemical Journal, 2019, 150, 104123	Quinazoline derivative (Off-on)	DMSO	1271 (6.34 μM)	Hg^{2+}
6.	Inorganic Chemistry Communications, 2018, 89, 46-50	Fluorescein based probe (Off-on)	MeOH:HEPES (5:95 v/v, 20 mM, pH 7.4)	22 (0.11 μM)	Hg^{2+}
7.	Anal. Methods, 2019, 11, 227–231	Terpyridine based probe (On-off)	Aqueous solution	138 (0.68 μM)	Hg^{2+}
8.	ACS Appl. Mater. Inter.,2017, 9, 13554–13563.	Eu(DPA)3@Lap-Tris/Cu2+ (Off-on)	hydrogel	49.78 (0.162 μM)	GSH
9.	Rsc Adv., 2016,6, 79526–79532.	MnO_2-Cu nanocomposites (Off-on)	-	30.73 (0.1 μM)	GSH
10.	Sensors and Actuators: B. Chemical., 2017, 251,753-762	Bromoacetyl bromide-functionalized CDs (Off-on)	PBS buffer (0.01 mol/L, pH = 8.0)	43 (0.14 μM)	GSH

References

1. H.A. Benesi. and J.H. Hildebrand, A spectrophotometric investigation of the interaction of iodine with aromatic hydrocarbons, J. Am. Chem. Soc., 1949, 71,2703-2707.

2. F. Han, Y. Bao, Z. Yang, T.M. Fyles, J. Zhao, X. Peng, J. Fan, Y. Wu, S. Sun, Simple bisthiocarbonohydrazones as sensitive selective, colorimetric, and switch-on fluorescent chemosensors for fluoride anions, Chem. Eur. J., 2007, 13, 2880-2892.

3. J. P. Nandre, S. R. Patil, S. K. Sahoo, C. P. Pradeep, A. Churakov, F.Yu, L. Chen, C. Redshaw, A. A. Patil and U. D. Patil, A chemosensor for micro- to nano-molar detection of Ag^{+} and Hg^{2+} ions in pure aqueous media and its applications in cell imaging ,Dalton Trans., 2017, 46, 14201–14209.